SLAC–PUB–6448
April 1994
(M)

SPIN DYNAMICS IN STORAGE RINGS AND LINEAR ACCELERATORS*

John Irwin
Stanford Linear Accelerator Center
Stanford University, Stanford, California 94309

ABSTRACT

The purpose of these lectures is to survey the subject of spin dynamics in accelerators: to give a sense of the underlying physics, the typical analytic and numeric methods used, and an overview of results achieved. Consideration will be limited to electrons and protons. Examples of experimental and theoretical results in both linear and circular machines are included.

Invited talk presented at the 21st Annual SLAC Summer Institute on Particle Physics: Spin Structures in High Energy Processes Stanford, CA, July 26–August 6, 1993.

⋆ Work supported by Department of Energy contract DE–AC03–76SF00515.

1 Spin Prelimnaries

1.1 2-D Spinors and Density Matrix

For spin 1/2 particles, such as the electron and proton, the spin observable is determined by a ray in a 2-D Hilbert space. Since the ray is normalized to unity and has an arbitray phase, two real numbers uniquely determine this ray. The standard choice of these two parameters, so as to give a one-to-one correspondence with the usual polar description of a unit directional vector in three dimensional space is:

$$\Psi_{\mathbf{n}} = e^{i\lambda} \begin{bmatrix} \cos(\theta/2)\, e^{-i\varphi/2} \\ \sin(\theta/2)\, e^{+i\varphi/2} \end{bmatrix} \leftrightarrow \mathbf{n} = (\sin\theta\cos\varphi, \sin\theta\sin\varphi, \cos\theta). \tag{1}$$

This correspondence may be extracted from the relationship:

$$\vec{n} = \langle \Psi_{\mathbf{n}} \vec{\sigma} \Psi_{\mathbf{n}} \rangle \,, \tag{2}$$

where the $\vec{\sigma}$ are the two-by-two traceless Hermitian Pauli spin matrices. The operators $-i\sigma_j/2$ generate rotations,

$$\frac{d\Psi_{\mathbf{n}}}{d\phi} = -\frac{i}{2}\vec{\sigma}\cdot\hat{\Phi}\,\Psi_{\mathbf{n}}, \tag{3}$$

and a Pauli matrix calculation confirms the desired relationship:

$$\frac{d\mathbf{n}}{d\phi} = \left\langle \frac{d\Psi_{\mathbf{n}}}{d\phi}\vec{\sigma}\Psi_{\mathbf{n}} \right\rangle + \left\langle \Psi_{\mathbf{n}}\vec{\sigma}\frac{d\Psi_{\mathbf{n}}}{d\phi} \right\rangle = \hat{\Phi}\times\mathbf{n}. \tag{4}$$

In quantum mechanics the rotation generator times $i\hbar$ is the angular momentum operator, hence it is usual to define a spin $\mathbf{S} = \hbar\vec{\sigma}/2$. The spin vector can couple with a classical magnetic field to give a scalar Hamiltonian. There is a free proportionality constant, and it is usual to define a magnetic moment $\vec{\mu} = ge/2m\mathbf{S}$, with the Hamiltonian given by $H = -\vec{\mu}\cdot\mathbf{B}$. For orbital angular momentum the proportionality constant is determined; $g = 1$, and $\vec{\mu} = e/2m\mathbf{L}$. The constant g is called the Lande g factor. For the electron $g \approx 2$.

The Hamiltonian is the generator of the time evolution,

$$\frac{d\Psi}{d\tau} = \frac{-i}{\hbar} H\Psi = \frac{ge}{2m}\left(\frac{i}{2}\vec{\sigma}\cdot\mathbf{B}\right)\Psi; \tag{5}$$

hence the direction vector $\mathbf{n}$ characterizing Ψ satisfies

$$\frac{d\mathbf{n}}{d\tau} = \mathbf{\Omega}_L \times \mathbf{n}, \quad \text{with} \quad \mathbf{\Omega}_L = \frac{-ge}{2m}\mathbf{B}. \tag{6}$$

The quantity $\mid \Omega_L \mid$ is called the Larmor precession frequency. The variable τ has been chosen to represent the time variable so as to draw attention to the fact that the frame of reference is taken to be the rest frame of the particle. The electron charge e is a negative quantity for the electron. The highest energy state for the electron has the spin aligned with the magnetic field. Note that even for a magnetic field of B = 1 Tesla, the energy $\hbar\Omega_L = 10^{-4}$ eV, which is much less than the kinetic energy of particles in accelerators. In other words, with very high accuracy the spin motion will have no influence on the particle orbit motion.

For an ensemble U and any observable $\mathbf{O}$, the expected value of $\mathbf{O}$ is given by

$$\langle \mathbf{O} \rangle = \langle\langle \Psi \mathbf{O} \Psi \rangle\rangle_{\Psi \in U} = \frac{1}{N} \sum_i n_i \langle \Psi_i \mathbf{O} \Psi_i \rangle, \tag{7}$$

where $N = \sum_i n_i$, and n_i is the number of occurences of Ψ_i in the ensemble. If each Ψ_i in the ensemble is expanded in some basis designated by Φ_m, $\Psi_i = \sum_m c_{im}\Phi_m$, and $\mathbf{O}$ is characterized by its matrix elements in this basis, $\mathbf{O}_{mn} = \langle \Phi_m \mathbf{O} \Phi_n \rangle$, then upon entering these expressions into the definition of $\langle \mathbf{O} \rangle$ the expected value of $\mathbf{O}$ is given by

$$\langle \mathbf{O} \rangle = \sum_{mn} \frac{1}{N} \sum_i n_i c_{in}^* c_{im} \mathbf{O}_{mn}. \tag{8}$$

All the information that is needed to characterize the ensemble is given by the matrix ρ with

$$\rho_{mn} = \frac{1}{N} \sum_i n_i c_{in}^* c_{im}. \tag{9}$$

This matrix ρ is called the density matrix. From its definition it can be deduced to be i) Hermitian, ii) positive, and iii) have Tr $\rho = 1$.

Since all 2 x 2 Hermitian matrices are given by four numbers, ρ can be expanded in the basis consisting of the unit matrix I and the three σ matrices. Since the σs are traceless and trace of ρ is unity, there are three unknown constants, and they may be chosen to be components of a vector according to

$$\rho = 1/2\,[I + (\mathbf{P}\cdot\sigma)]\,. \tag{10}$$

If the basis states defining ρ are rotated so that the z-axis is in the direction of $\mathbf{P}$, then

$$\rho = \begin{bmatrix} (1+P_z)/2 & 0 \\ 0 & (1-P_z)/2 \end{bmatrix}, \tag{11}$$

and one can see that the positivity of ρ implies that $\mid \mathbf{P} \mid \leq 1$. Further since it may be verified that

$$d\mathbf{P}/d\tau = \mathbf{\Omega}_L \times \mathbf{P}, \tag{12}$$

it is appropriate to interpret $\mathbf{P}$ as the polarization of the ensemble.

1.2 Thomas-BMT Equation[1]

If the particle orbit is given, then $B(\tau)$ can be found from $B(t)$ by transforming to the rest frame of the particle. Such frames can be obtained by pure boosts from the lab frame. If a particle is moving along an orbit, such that in time δt the velocity has changed $\delta\mathbf{v}$, from $\mathbf{v}_1$ to $\mathbf{v}_2 = \mathbf{v}_1 + \delta\mathbf{v}$, Thomas[2] noted that if O_1 was a frame of reference at rest with respect to the particle at time t_1 obtained by a boost from the lab frame, and O_2 was a frame of reference at rest with respect to the particle at time t_2 also obtained by a boost from the lab frame, and if O_2' was a frame of reference at rest with respect to the particle at time t_2 obtained by a boost from the frame O_1, then O_2' is rotated with respect to O_2 by an amount

$$\delta\theta_{\mathrm{LP}} = -\,(\gamma - 1)\,\delta\theta_{\mathrm{O}}. \tag{13}$$

(LP signifies "as seen from the pure boost frames from lab", and O signifies rotation of orbit direction.) Thus in a sequence of pure boost frames, each at rest with respect to the particle, a constant vector in the rest frame of the particle will appear to precess in a sense opposite to the rotation determined by the sequence of velocity vectors in the lab frame.

Assuming for the moment that the particle is moving in a magnetic field, then

$$d\mathbf{v}/dt = e/m\gamma\,(\mathbf{v}\times\mathbf{B})\,. \tag{14}$$

The magnetic field in the pure boost frames at rest with respect to the particle would have a field in those frames of

$$\mathbf{B}_{LP} = \gamma\mathbf{B}_\perp + \mathbf{B}_\parallel \tag{15}$$

($\perp$ indicates the component perpendicular to and $\parallel$ the component parallel to the velocity vector). The precesion frequency in the sequence of lab frames (use $d\tau = dt/\gamma$) would be

$$\mathbf{\Omega}_{LP} = -g\frac{e}{2m}\left(\mathbf{B}_\perp + \frac{1}{\gamma}\mathbf{B}_\parallel\right). \tag{16}$$

However in this set of frames, even were it constant, the spin would appear to precess at the frequency (T for Thomas)

$$\mathbf{\Omega}_{TP} = (\gamma-1)\,\frac{e}{m\gamma}\mathbf{B}_\perp. \tag{17}$$

The sum of these gives an apparent precession frequency of

$$\mathbf{\Omega}_{TLP} = -\frac{e}{m}\left[\left(a+\frac{1}{\gamma}\right)\mathbf{B}_\perp + \frac{a+1}{\gamma}\mathbf{B}_\parallel\right], \tag{18}$$

where $a = (g-2)/2 \approx 1.16\times10^{-3}$ for electrons, and $a \approx 1.79$ for protons.

If an electric field is present the apparent rotation frequency is

$$\mathbf{\Omega}_{TLP} = -\frac{e}{m}\left[\left(a+\frac{1}{\gamma}\right)\mathbf{B}_\perp + \frac{a+1}{\gamma}\mathbf{B}_\parallel - \left(a+\frac{1}{\gamma+1}\right)\frac{\mathbf{v}\times\mathbf{E}}{c^2}\right]. \tag{19}$$

The dominant term here is usually $a\mathbf{B}_\perp$. The $\mathbf{B}_\parallel$ can be significant at low energies for particles in a solenoid. The last term is usually small for two reasons: typically $E/c \ll B$ (a 1-Tesla magnetic field has a strength equivalent to an electric field of 3 MV/cm), and very often E is parallel to $\mathbf{v}$.

In a constant magnetic field in the labratory with motion given by $d\mathbf{v}/dt = e/m\gamma(\mathbf{v} \times \mathbf{B})$, a frame in the laboratory that rotates so that one axis is always pointing in the direction of the velocity, rotates with a frequency called the cyclotron frequency,

$$\mathbf{\Omega}_C = -\frac{e}{m\gamma}\mathbf{B}_\perp. \tag{20}$$

If one observes the precession of the particle spin in frames of reference that are pure boosts from this rotating frame in the lab, then the $1/\gamma$ $\mathbf{B}_\perp$ cancels out. Observed from this sequence of frames, and assuming a field perpendicular to the velocity vector,

$$\mathbf{\Omega}_{TLPO} = \gamma a \mathbf{\Omega}_C \tag{21}$$

(TLPO signifies a rotation observed in frames which are pure boosts from a lab frame rotating with the orbit, accounting for the Thomas precession effect). We have the very simple result that the spin in these frames rotates γa times as fast as the orbit rotation, *i.e.,* for one orbit around an accelerator, the spin would precess γa times. This result is usually valid when other fields are present because the other terms are very small. For electrons $\gamma a = E(GeV)/0.44065$, and for protons $\gamma a = E(GeV)/0.52335$, so for similar energies, the rotation angle of protons and electrons is similar. The product γa is called the spin tune. It is interesting to note that the proportionality between the orbit change and the spin precession gives a sense of the "stiffness" of the spin. The orbit has to be substantially altered in order to alter the spin direction.

For a particle in a circular accelerator, travelling in a horizontal plane with dipole fields in the vertical direction, there will be horizontal fields from imperfections and from focussing in the quadrupoles. These fields usually average to zero, are weak, and act over short distances. However if these horizontal fields occur with a frequency that matches the spin frequency, they can cause the direction of the spin to change. This condition is called a spin resonance and is discussed in detail in Section 4.4.

1.3 Spinor representation of classical precession

Since the precesion equation $d\mathbf{n}/dt = \mathbf{\Omega} \times \mathbf{n}$, with $\mathbf{\Omega} = -ge/2m\mathbf{B}$, describes the motion of the direction of the 2-D Hilbert space vector $\Psi_{\mathbf{n}}$ under the action of the generator $G = -i\vec{\sigma} \cdot \mathbf{\Omega}/2$, it is acceptable and indeed often convenient to analyze precessional motion by solving spinor equations. In anticpation of this use, and assuming the precession equation to be analyzed is $d\mathbf{n}/dt = \mathbf{\Omega}_{TLPO} \times \mathbf{n}$, the generator is given by

$$\begin{aligned} G &= -\tfrac{i}{2}\vec{\sigma} \cdot \mathbf{\Omega}_{TLPO} \\ &= \tfrac{ie}{m\gamma} \begin{bmatrix} \gamma a B_z & (1+\gamma a)\, B_x - i\,(1+a)\, B_s \\ (1+\gamma a)\, B_x + i\,(1+a)\, B_s & -\gamma a B_z \end{bmatrix}, \end{aligned} \tag{22}$$

which for large γ becomes

$$G = -\frac{i}{2}\vec{\sigma} \cdot \mathbf{\Omega}_{TLPO} = \frac{iea}{m} \begin{bmatrix} B_z & B_x \\ B_x & -B_z \end{bmatrix}. \tag{23}$$

2 Accelerator Physics Preliminaries

2.1 Linear Transport and Closed Orbit

The typical elements of an accelerator are: i) dipoles which have a constant magnetic field to bend the beam; ii) quadrupoles which have a linear field ($B_y = kx, B_x = -ky$) used to focus the beam; iii) sextupole pairs for chromatic corrections; and, rarely, iv) octupoles for tune-shift-with-amplitude or other minor orbit adjustments. The fringe fields of dipoles have a sextupole-like quality, and the fringe fields of quadrupoles have an octupole-like quality. Since the sextupoles occur in pairs, in such a way that the sextupole aberrations cancel, and the octupoles are very weak, it will be satisfactory for a first analysis to limit the discussion to dipoles and quadrupoles.

The effect of a linear element, such as a drift or quadrupole, may be represented by a matrix. If the phase space state of a particle is represented by the

four vector $\mathbf{z} = (x, x', y, y')$, then passage through a drift is represented by

$$\mathbf{z}_2 = \mathbf{M}_L \mathbf{z}_1, \tag{24}$$

where M_L is given by

$$M_L = \begin{bmatrix} 1 & L & 0 & 0 \\ 0 & 1 & 0 & 0 \\ 0 & 0 & 1 & L \\ 0 & 0 & 0 & 1 \end{bmatrix}.$$

A thin quadrupole kick can be represented by the matrix

$$M_Q = \begin{bmatrix} 1 & 0 & 0 & 0 \\ -k & 1 & 0 & 0 \\ 0 & 0 & 1 & 0 \\ 0 & 0 & k & 1 \end{bmatrix}. \tag{25}$$

Each of these matrices has unit determinant and is symplectic. Thick quadrupoles can be represented by a sequence of drifts and thin kicks, hence beam lines made up of drifts and thick quadrupoles can be represented by products of the above matrices. A tilted quad, indeed any linear transformation, may be represented by a matrix.

Being a product of symplectic matrices, the one turn matrix of a storage ring is necessarily symplectic. If λ is an eigenvalue of a symplectic matrix, so is $1/\lambda$, and since these are real matrices, so is its complex conjugate λ^*. Taking $\lambda = e^{\mu}$, it follows that μ is either real or purely immaginary. Real μ unequal to zero is excluded, for in such a case there would be an initial coordinate that would become arbitrarily large after many turns. The pure complex case corresponds to a stable ring.

The real and imaginary parts of the eigenvectors of the one turn matrix M can be used to define a simlarity transformation A which has the property

$$M = \mathbf{A}^{-1} \begin{bmatrix} \cos\mu_x & \sin\mu_x & 0 & 0 \\ -\sin\mu_x & \cos\mu_x & 0 & 0 \\ 0 & 0 & \cos\mu_y & \sin\mu_y \\ 0 & 0 & -\sin\mu_y & \cos\mu_y \end{bmatrix} \mathbf{A}. \tag{26}$$

Though the one turn matrix is a function of the starting place in the ring, all one turn matrices are related by a similarity transformation, namely the transport

matrix between the two starting points. Hence the eigenvalues of the one turn matrix will not depend on the location at which the one-turn map is defined. The quantities $\nu_{x,y} = \mu_{x,y}/2\pi$ are called the tunes of the ring.

The dipole strengths are chosen to define a closed orbit at the design energy. However errors in dipole strengths and quadrupole mis-alignments will cause the design orbit not to close exactly. However if the ring is stable, a closed orbit can be found. Suppose after one turn the image of a particle represented by initial coordinates $\mathbf{a}$ maps to the point $\mathbf{b}$, then the point $\mathbf{a}+\Delta\mathbf{a}$ will map into $\mathbf{b}+M\Delta\mathbf{a}$, where M is the one-turn matrix. To find a fixed point it is necessary to solve

$$\mathbf{a}+\Delta\mathbf{a} = \mathbf{b}+M\Delta\mathbf{a}, \quad \text{or} \quad (1-M)\,\Delta\mathbf{a} = \mathbf{b}-\mathbf{a}. \tag{27}$$

If unity is excluded as an eigenvalue, the matrix (1-M) is invertible, and a fixed point can be found. The fixed point, and its image around the ring, is called the "closed orbit".

2.2 Betatron and Synchrotron Oscillations

After redefining the coordinate system so that the closed orbit is at the origin, there exist four independent solutions, two for primarily horizontal motion and two for vertical motion. In each pair there is one sine-like and one cosine-like solution. These are defined as

$$\begin{aligned} z_1(s) &= M(s)\,\mathbf{A}^{-1}(1,0,0,0); \\ z_2(s) &= M(s)\,\mathbf{A}^{-1}(0,1,0,0); \\ z_3(s) &= M(s)\,\mathbf{A}^{-1}(0,0,1,0); \\ z_4(s) &= M(s)\,\mathbf{A}^{-1}(0,0,0,1); \end{aligned} \tag{28}$$

where M(s) is the tranport matrix from the initial plane to a point a distance s along the closed orbit, and A is the simlarity matrix defined above. For $nC < s < (n+1)C$, where C is the circumference of the closed orbit, it follows from this definition that

$$\begin{aligned} z_1(s) &= \cos(n\mu_x)\,z_1(\tilde{s}) + \sin(n\mu_x)\,z_2(\tilde{s}); \\ z_2(s) &= -\sin(n\mu_x)\,z_1(\tilde{s}) + \cos(n\mu_x)\,z_2(\tilde{s}); \\ z_3(s) &= \cos(n\mu_y)\,z_3(\tilde{s}) + \sin(n\mu_y)\,z_4(\tilde{s}); \\ z_4(s) &= -\sin(n\mu_y)\,z_3(\tilde{s}) + \cos(n\mu_y)\,z_4(\tilde{s}). \end{aligned} \tag{29}$$

where $\tilde{s} = s - nC$ is between 0 and C. In other words only the functional form of the four functions on the first turn is required to determine the orbit for all later

turns. These oscillations of the particle around the closed orbit are called betatron oscillations. Depending on intial coordinates the motion is a linear combination of the four $\mathbf{z}_k(\mathrm{s})$.

There also exist non-zero energy spread and bunch length. It is possible to introduce two additional coordinates: 1) $\delta = \delta E/E$, the fractional departure from the design energy, and 2) $c\tau = \Delta s$, the longitudinal distance from the center of the bunch. Particles oscillate about the design energy and about the center of the bunch, and oscillations in this third degree of freedom are called synchrotron oscillations. The closed orbit is slightly dependent on energy, defining a function called the dispersion function, and there is a tune associated with the synchrotron motion which is typically much smaller than the betatron tunes. This fact allows the synchrotron motion to be treated as a modulation of the betatron oscillations and leads to "sideband" phenomena.

3 Linear Accelerators

Figure 1 shows the layout of the Stanford Linear Accelerator (SLC). The polarized electron source is at the bottom of the figure. The arrows along the electron beam line indicate the direction of the polarization as the beam proceeds from the source through the pre-accelerator to the damping ring, then from the damping ring to the main accelerator, and finally to the north arc and the IP at the top of the figure.

3.1 Space Charge Depolarization in Injector

For the space charge fields of cylindrical bunches (assuming no external fields)

$$\mathbf{B} = \mathbf{v} \times \mathbf{E}/c^2, \quad \text{and} \quad \mathbf{v} \cdot \mathbf{B} = 0. \tag{30}$$

hence $\mathbf{B}_{\|} = 0$, and remaining terms proportional to "a" cancel, leaving

$$\mathbf{\Omega} = -\frac{e}{m}\left(\frac{1}{\gamma} - \frac{1}{\gamma+1}\right)\mathbf{B}_{\perp} = -\frac{e}{m}\frac{1}{\gamma\,(\gamma+1)}\mathbf{B}_{\perp}. \tag{31}$$

This diminishes rapidly with increasing γ. Furthermore, since lines of $\mathbf{B}$ circle the bunch and particle orbits oscillate back and forth across the bunch, the spin

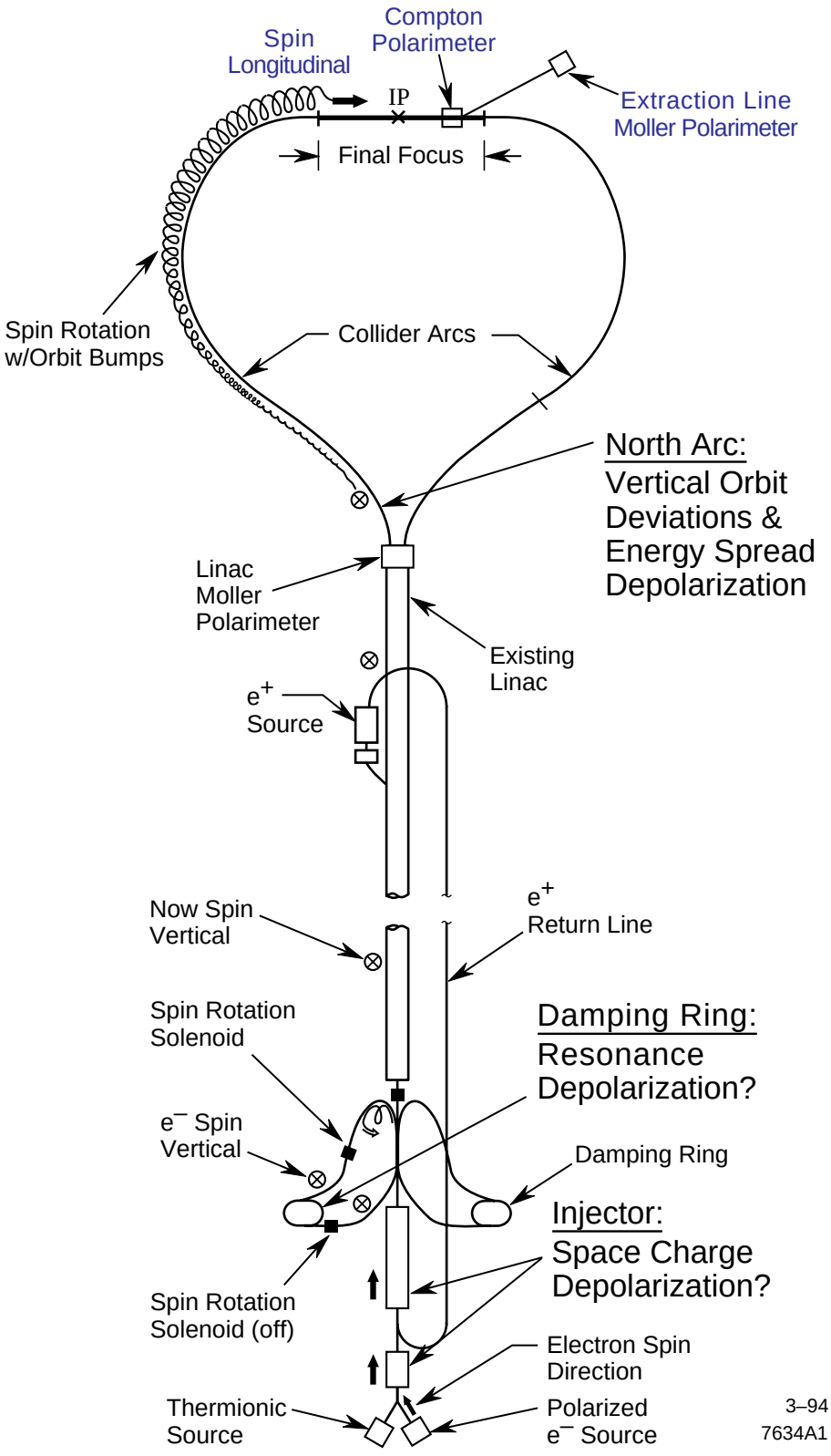

Figure 1. Schematic layout of SLC showing direction of spin polarization as of '93 for the flat beam configuration.

rotation direction changes sign and may cancel out. However, neglecting this cancelation it is possible to estimate the rotation angle.

$$|\Omega|_{\max} = \frac{e\,|B_\phi|}{m\gamma\,(\gamma+1)} \approx \frac{0.3 N r_e v}{\sigma_r \sigma_z \gamma\,(\gamma+1)}. \tag{32}$$

The calculation of the maximum possible precession in the pre-accelerator, after the injector, is given by Ref. 3:

$$\begin{aligned} \Delta\phi_{\max} &= \Omega_{\max} dt = \Omega dz/v \le 0.3 N r_e/(\sigma_r \sigma_z d\gamma/dz) \quad d\gamma/\gamma^2 \\ &\approx 0.06\left[1/\gamma_i - 1/\gamma_f\right] < 0.006, \end{aligned} \tag{33}$$

where $r_e = 2.8\times10^{-15}$ m, $\sigma_r = 4$ mm, $\sigma_z = 2$ mm, $N = 5\times10^{10}$, $\gamma_i = 100$, $\gamma_f = 2\times 10^3$, and $d\gamma/dz = 30\mathrm{m}^{-1}$. One can conclude that there is no spin precession from space charge after $\gamma = 100$. Similar estimates for the injector region ($\gamma_i < 100$) are shown in Fig. 2, where the bunch length is shown as a function of position. The conclusion is that the total $\Delta\phi_{max} < 0.06$. Averaging over the radius of beam yields a remaining polarization of at least $\langle P\rangle \ge 0.9 P_{source}$. This is a comforatable situation since no cancellations were assumed.

3.2 Spin Manipulation into Damping Ring

Figure 3 shows the region following the pre-accelerator, leading to and from the electron damping ring. Since $\gamma a = 2.74$ at the end of the pre-accelerator, the polarization direction is rotated by 90° when the beam direction is rotated by 32.8°. The bend into the RTL (ring-to-linac transport line) has been chosen to be five times 32.8° so that the polarization is perpendicular to the direction of motion. This bend is followed by a straight section of beam line containing a solenoid. The magnitude of the field in the solenoid is chosen so that the polarization is rotated into the vertical direction. Thus the polarization is not affected by the subsequent bend, and the beam enters the damping ring vertically polarized. This is essential if the polarization is to be preserved in the damping ring where the beam travels many revolutions and the energy spread would cause a complete depolarization for horizontal polarization. The details of spin dynamics in the damping ring are treated after a discussion of the spin dynamics of the north arc.

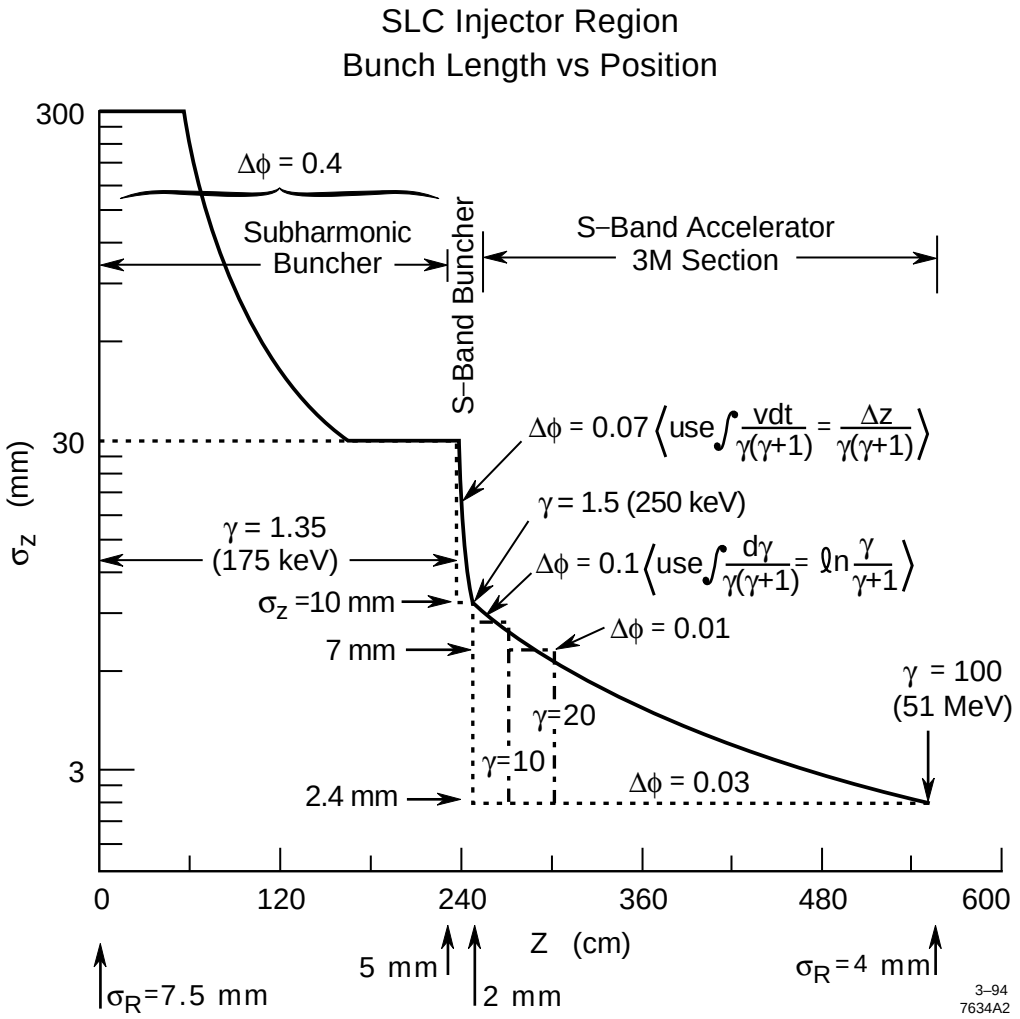

Figure 2. The bunch length and the maximum precession phase due to space charge in the SLC injector.[3]

3.3 Spin Rotation in SLC North Arc

In a planar ring or arc on the design orbit a particle would experience only a vertical bending field ($B_x = B_s = 0$), and

$$\frac{d\mathbf{n}}{dt} = \mathbf{\Omega}_{TLPO} \times \mathbf{n} = \gamma a \mathbf{\Omega}_C \times \mathbf{n} = \gamma a \frac{c}{\rho\,(s)} \hat{\mathbf{z}} \times \mathbf{n} \tag{34}$$

($\hat{\mathbf{z}}$ is taken as a unit vector in the vertical direction, rather than $\hat{\mathbf{y}}$, since the conventions for spin usually have $\hat{\mathbf{z}}$ as the polarization axis). Converting c dt to ds and letting $ds/\rho(s) = d\theta$ be the change in direction of the orbit, the above equation can be rewritten as

$$\frac{d\mathbf{n}}{d\theta} = \gamma a \hat{\mathbf{z}} \times \mathbf{n} = \nu_{sp} \hat{\mathbf{z}} \times \mathbf{n}, \tag{35}$$

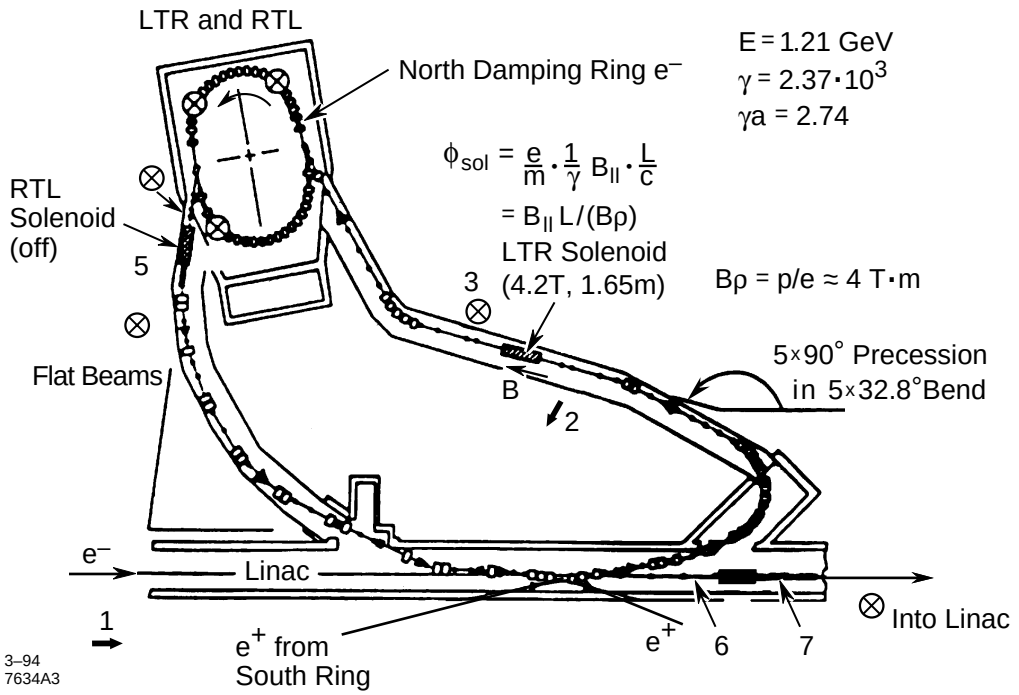

Figure 3. An enlargement of the SLC north daming ring and the linac-to-ring(LTR) and ring-to-linac (RTL) transport lines showing the direction of spin polarization for the flat beam configuration.

where ν_{sp} is the tune spin, and $\nu_{sp} = 100$ in the north arc.

Now add some small B_x in resonance with the spin precession. Without B_x the spin just precesses about the z direction, but with a "resonant" B_x the set of motions sketched in Fig. 4 may be realized. Even with a relatively small B_x, this situation can result in spin flip. Figure 5 shows a particle orbit in the SLC north arc that results from a small vertical kick, and shown superimposed is a plot of the horizontal component of the spin. Note that, by a lucky coincidence, the spin precesses one time in exactly an arc length corresponding to one vertical betatron oscillation. When the particle is at a maximum in its trajectory, the quadrupole field is bending the particle back toward the midplane, and since the spin at these locations always has the same orientation, the resonant condition sketched in the above sequence of drawings applies. Figure 5 also shows the slow growth of the vertical component of the spin that results from this resonant condition. By adjusting two vertical bumps in the last section of the north arc, it has been possible to completely control the polarization orientation at the IP.

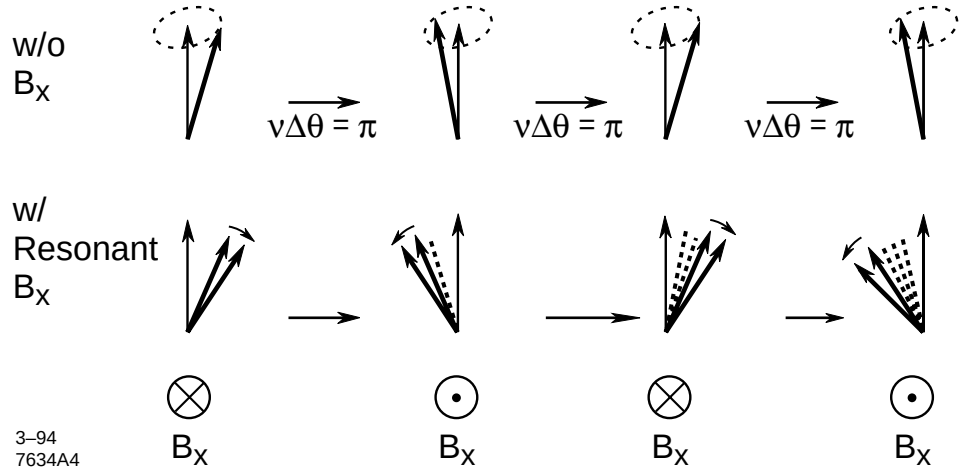

Figure 4. Spin moves away from the precession axis under the influence of a horizontal magnetic field which changes in phase along with the with the precession rate. This condition is called spin "resonance" condition.

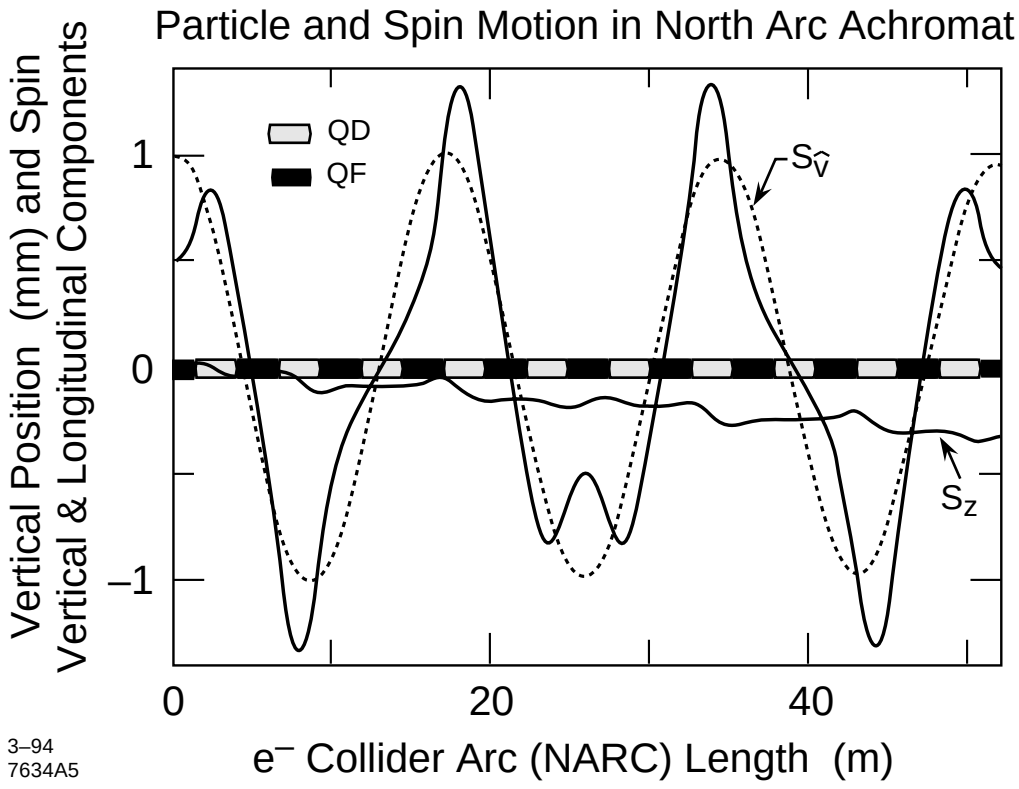

Figure 5. A graph of both a vertical betatron orbit and a horizontal component of the spin vector in the SLC north arc indicating that the resonance condition is very well satisfied there.[4]

This situation can be analyzed quite nicely using the spinor representation for the precession equation, as described in Section 2.3. Without B_x the spinor equation is

$$\frac{d\Psi}{d\theta} = \frac{-i\gamma a}{2}\begin{bmatrix} 1 & 0 \\ 0 & -1 \end{bmatrix}\Psi(\theta), \tag{36}$$

which has the solution

$$\Psi(\theta) = \exp\left(\frac{-i\gamma a\theta}{2}\sigma_z\right)\cdot\Psi(0). \tag{37}$$

With B_x the equation is

$$\frac{d\Psi}{d\theta} = \frac{-i\gamma a}{2}\begin{bmatrix} 1 & -e\rho(\theta)B_x(\theta)/p \\ -e\rho(\theta)B_x(\theta)/p & -1 \end{bmatrix}\Psi(\theta), \tag{38}$$

where p is the longitudinal momentum, and p/e is often referred to as the magnetic rigidity $B\rho$. It could arise that a quadrupole with $B_x \neq 0$ is located in a straight section where θ does not advance. Then $\rho d\theta = ds$, and it is necessary to integrate $B_x(s)$ along the trajectory through the straight region. If the off diagonal element is Fourier analyzed on the particle orbit

$$\frac{e\gamma a\cdot\rho(\theta)B_x(\theta)}{p} = \sum_{k=-\infty}^{\infty}\varepsilon_k e^{-ik\theta}, \tag{39}$$

and one term is dominant; the equation for Ψ then becomes

$$\frac{d\Psi}{d\theta} = \frac{i\gamma a}{2}\begin{bmatrix} 1 & -\varepsilon_k e^{-ik\theta} \\ -\varepsilon_k^* e^{ik\theta} & -1 \end{bmatrix}\Psi(\theta). \tag{40}$$

Note that $B_x(\theta)$ can come from either imperfections in the lattice or from betatron oscillations as described above. To solve this equation it is convenient to move to a co-rotating frame by substituting

$$\Psi(\theta) = \exp\left(\frac{-ik\theta}{2}\sigma_z\right)\cdot\Phi(\theta) \tag{41}$$

resulting in an equation for Φ:

$$\frac{d\Phi}{d\theta} = -i\begin{bmatrix} -\Delta & -\varepsilon_k \\ -\varepsilon_k^* & \Delta \end{bmatrix}\Phi(\theta) = \frac{-i}{2}\vec{\sigma}\cdot\vec{\lambda}\Phi(\theta), \tag{42}$$

where $\lambda_z = \Delta = \nu_{sp} - k$, $\lambda_x = Re(\varepsilon)$, $\lambda_y = Im(\varepsilon)$, and $\mid\vec{\lambda}\mid = \sqrt{\Delta^2+\varepsilon^2}$. This

may be solved to yield

$$\Phi(\theta) = exp(-i\vec{\sigma} \cdot \vec{\lambda}\theta/2)\Phi(0). \tag{43}$$

Thus the resultant motion is a precession about the direction $\vec{\lambda}$ with frequency $\mid \vec{\lambda} \mid$, which all is precessing about $\hat{\mathbf{z}}$. Letting ξ be the polar angle of $\vec{\lambda}$, then $\cos\xi = \Delta/\sqrt{\Delta^2 + \varepsilon^2}$ has the value +1 for large positive Δ, −1 for large negative Δ, and is 0 for $\Delta = 0$ (exactly on resonance). If the spin tune is changed "slowly", say by changing the energy, so that Δ moves from +1 to –1, then a particle whose spin is primarily in the +z direction will precess about $\vec{\lambda}$ as $\vec{\lambda}$ moves from the +z to the –z direction. The spin will end up pointing in the –z direction. The width of this "resonance" region is seen to be about 2ε. "Slowly" changing the spin tune should be interpreted to mean that the change of Δ from $-\varepsilon$ to $+\varepsilon$ should require many oscillations. Letting $d\nu/d\theta = \alpha$, the resonance passage would occur in $\Delta\theta = 2\varepsilon/\alpha$. Many oscillations would require $\mid \lambda \mid \Delta\theta \gg 2\pi$. Since $\mid \lambda \mid \geq \varepsilon$, this condition may be written $\alpha \ll \varepsilon^2/\pi$.

3.4 Damping Ring Considerations

Particles enter the damping ring with large betatron amplitudes and are damped through the mechanism of synchrotron radiation followed by energy make-up. Polarization or depolarization that can occur through the radiation process is discussed in Section 6.2. It is a slow process compared to the several damping times which electrons spend in the damping ring. Hence the resonant analysis described in the previous section is sufficient to understand the behavior of particles in the SLC damping ring. To understand the behavior of the spin we must analyze the function $B_x(\theta)$. Following Courant and Ruth,[5] this can be found by analyzing the particle orbit:

$$eB_x/p = eB_x c/pc = (dp_z/dt)/pc = (dp_z/ds)/p = d^2z/ds^2. \tag{44}$$

The last equality made use of the relationship $p_z/p = dz/ds$. Hence to find the Fourier analysis of the off-diagonal element, one may Fourier analyze d^2z/ds^2.

Resonances arising from the betatron motion are called intrinsic resonances, and resonances arising from machine errors are called imperfection resonances.

The imperfection resonances can cause a vertical excursion of the closed orbit. A Fourier analysis of the closed orbit could have components at any integer. For the betatron motion z(s), it was shown in Section 2.2 that on the nth turn

$$z\left(s\right)=\cos\left(n\mu_z\right)z_1\left(\tilde{s}\right)z_0+\sin\left(n\mu_z\right)z_2\left(\tilde{s}\right)z_0', \tag{45}$$

where z_0 and z_0' are the initial position and slope, $z_1(\tilde{s})$ and $z_2(\tilde{s})$ are the cosine-like and sine-like orbits on the first turn, $0\leq\tilde{s}=s-nC<C$ (C being the circumference), and μ_z is the betatron phase advance of each turn associated with motion in the z (vertical) direction. The fourier integral required is

$$\begin{aligned}&\int_{-\infty}^{\infty}e^{-i\kappa\theta}\rho\left(\theta\right)z''\left(\theta\right)d\theta\\&=\left(\sum_n e^{-i\kappa 2\pi n}\cos\left(n\mu_z\right)\right)\int_0^{2\pi}e^{-i\kappa\theta}\rho\left(\theta\right)z_1''\left(\theta\right)d\theta+\ldots\\&=\left(\sum_m\delta\left(\kappa\pm\tfrac{\mu_z}{2\pi}+m\right)\right)\int_0^{2\pi}e^{-i\kappa\theta}\rho\left(\theta\right)z_1''\left(\theta\right)d\theta+\ldots\end{aligned} \tag{46}$$

Therefore there are resonances at $\nu_{sp}=\kappa=\pm\mu_z/2\pi+m=\pm\nu_z+m$, for m any positive or negative integer, where ν_z is the tune of the vertical betatron motion.

Figure 6 shows what would be expected if the damping ring energy (spin tune) were near a resonance. Assuming the spin was in the z direction upon injection into the ring, it would then begin to precess about some vector $\vec{\lambda}_i$. This vector would precess about the z axis. When the particle is ejected from the ring, $\vec{\lambda}_i$ will have precessed to some final vector $\vec{\lambda}_f$, which without damping would have the same polar angle with respect to the z axis. However, the particle spin which is precessing now about $\vec{\lambda}_f$ will not usually be pointing in the z direction, and so the component of the spin in the z direction is generally smaller at extraction than on injection. In the presence of damping the amplitude of the betatron oscillation is reduced, so the resonance strength changes, and the polar angle of $\vec{\lambda}_f$ will adiabatically change, as indicated in Fig. 6.

Figure 7 shows a simlulation of the exit polarization expected as a function of the spin tune in the neighborhood of the design spin tune (≈ 2.7). Experimentally the polarization can be measured at the end of the main linac with a Moeller polarimeter. The beam can be sent directly down the linac from the injector or sent into the damping ring to be damped. Experimentally no decrease in polarization is observed from passage through the damping ring.

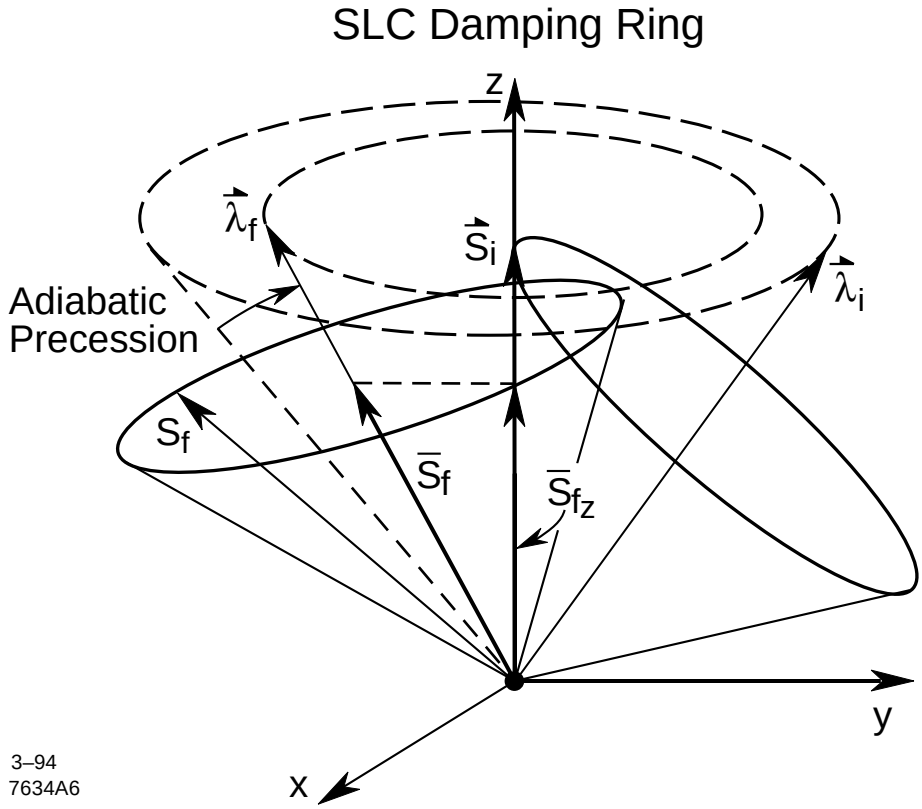

Figure 6. A sketch of the entry and exit polararization for the SLC damping ring illustrating that near a resonant condition the exit polarization will be less than the entry polarization.[6]

4 Proton Rings

In proton rings there is no polarization mechanism, as there often is in electron rings (see Section 6), so the only hope for having polarized beams is to polarize the beam at its source and preserve the polarization through the entire acceleration cycle. Since the spin tune changes with energy, many resonances are crossed. This section discusses the various methods that have been devised to cross resonances without losing beam polarization.

4.1 Resonance Crossing

We have already noticed that as the spin tune passes through a resonance the $\vec{\lambda}$ vector changes sign, from up to down, or vice-versa. If the resonances are crossed slowly the polarization will follow the $\vec{\lambda}$ vector, so the beam will remain polarized having only changed the sign of the polarization. This strategy has been used successfully. The main problem with this method is that the weak resonances must be crossed very slowly, and there are just too many resonances: one resonance every 0.52 GeV for a 10 TeV accelerator amounts to 20,000 resonances to cross.

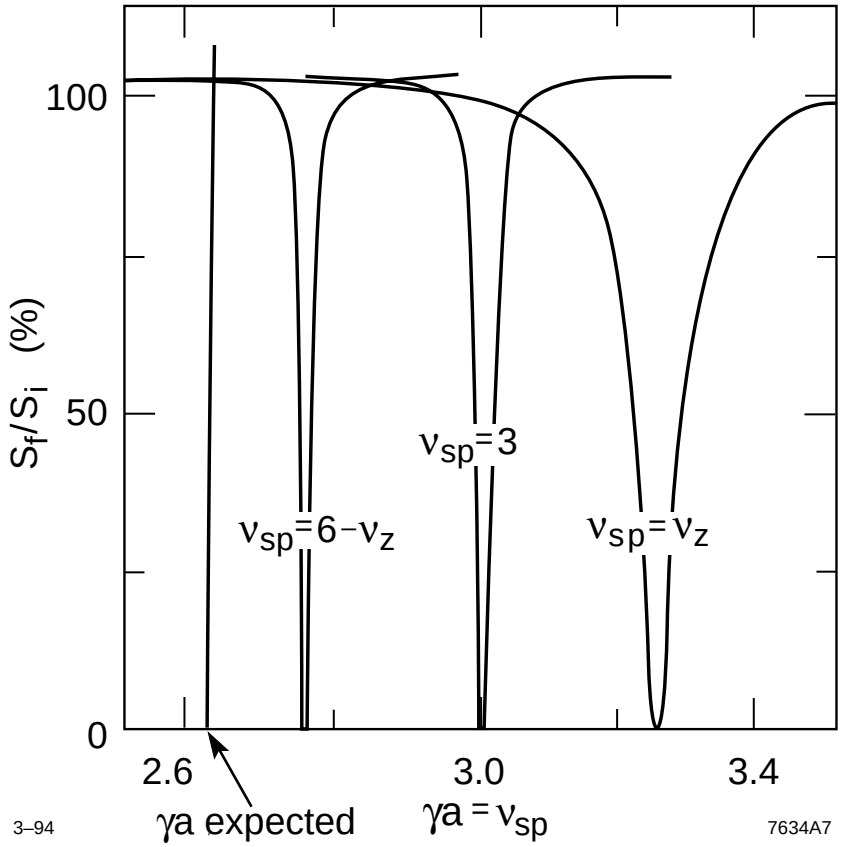

Figure 7. The results of a simulation of the exit polarization from the SLC damping ring as a funtion of spin tune (which is proporional to damping ring energy). The design tune spin is indicated. The potential depolarization from three separate resonants is evident.[6]

Froissart and Stora[7] were able to exactly solve the equations for passage through a resonance assuming a constant $\alpha = d\nu/d\theta$. They found

$$\frac{P_z\left(+\infty\right)}{P_z\left(-\infty\right)} = 2\exp\left(-\frac{\pi\varepsilon^2}{2\alpha}\right) - 1. \tag{47}$$

This shows that for very fast passage through a resonance ($d\nu/d\theta \gg \pi\varepsilon^2/2$) the polarization is not changed. This strategy has also been used succesfully. However the problem with higher energy accelerators is that the strength of the resonances increases to values greater than unity.

The resonant strength is proportional to the integral

$$\varepsilon \sim \int_0^{2\pi} e^{-i\kappa\theta}\rho\left(\theta\right)B_x\left(\theta\right)d\theta, \tag{48}$$

which is just the integrated strength of the B_x field along the orbit. The B_x field arises primarily in quadrupoles. The inverse focal length of the quadupole is given

by

$$\frac{1}{f} = \frac{eB_T L_Q}{ap}, \tag{49}$$

where p is the particle momentum, a is the quadrupole aperture, B_T is the pole tip field, and L_Q is the length. The number of quadrupoles in the ring is proportional to C/f, the circumference divided by the focal length of the quadrupoles. The field experienced by the particle will be the gradient times the vertical offset of the particle from the quadrupole axis. Putting this together

$$\begin{aligned} e^{-i\kappa\theta}\rho\left(\theta\right)B_x\left(\theta\right)d\theta = \quad & e^{i\kappa\theta(s)}B_x\left(s\right)ds \\ \sim \Delta z\tfrac{B_T}{a}L_Q C \sim \Delta z\gamma\tfrac{C}{f}, & \end{aligned} \tag{50}$$

where we have taken $B_x = \Delta z B_T/a$, which can be non-zero for a length L_Q. The number of such contributions can be C/f. With random signs the integral should increase like $\sqrt{C/f}$. As machines get larger C/f increases, but in a given machine where C and f are constant one expects the imperfection resonances to increase linearly with energy ($\varepsilon_{imp} \sim \gamma$), since Δz arises from vertically displaced quadrupoles and is constant. For the intrinsic resonances, Δz is the amplitude of the betatron oscillations. Since the emittance decreases with energy, this amplitude decreases like $1/\sqrt{\gamma}$. Hence $\varepsilon_{int} \sim \sqrt{\gamma}$. These estimates are evident in the calculations assembled in Fig. 8. Note that for the SSC the imperfection resonances have a strength of 10 to 100. Since imperfection resonances occur at every integer, the resonances will be highly overlapping, and the theory of Froissart and Stora is not applicable.

Imperfection resonances have been eliminated by putting in small closed orbit bumps with the right periodic structure until the strength of the resonance is compensated by the bump (harmonic matching). However for high energies, there are just too many resonances. They overlap, and none of these techniques is adequate.

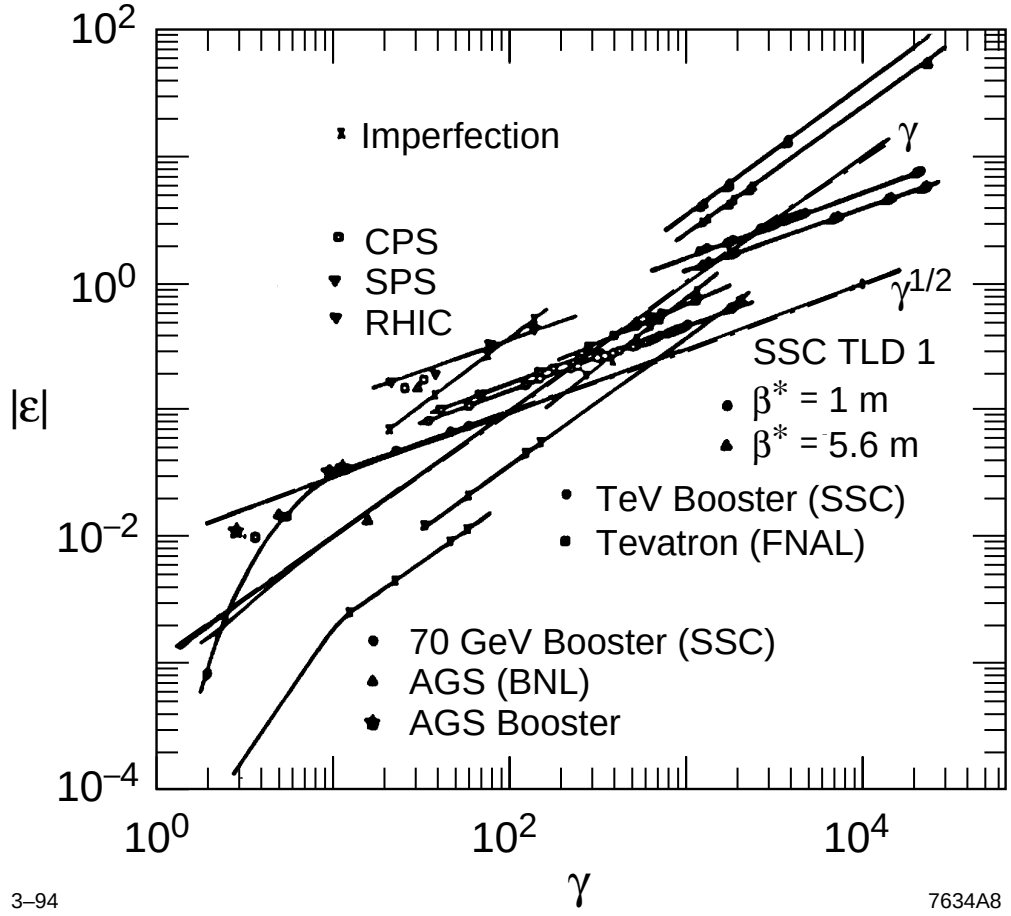

Figure 8. A compilation of the intrinsic and imperfection resonance strengths for several proton accelerators. Note that in any given machine the imperfection resonance strengths scale with energy and the intrinsic resonance strengths scale with the square root of energy.[8]

4.2 Siberian Snakes

Consider a particle moving along the closed orbit of a storage ring. Because of imperfections, or because of the presence of spin rotators sometimes inserted to ensure spin in the direction of the beam at interaction points, the spin is not always vertical. For one turn we may write

$$\Psi\left(\theta + 2\pi\right) = M\left(\theta\right)\Psi\left(\theta\right), \tag{51}$$

where $M(\theta)$ is the one turn matrix for the spin precesion, beginning and ending at the location designated by θ. It is clearly possible to find such a matrix because there is a spin transport matrix for every element of the ring, and the rotation for the complete ring will be given by the product of these matrices. Now every rotation can be characterized by an axis of rotation and an angle of rotation. The

angle of rotation will be the same for all θ since i) the rotation angle is given by the eigenvalues of the matrix, and ii) the one turn matrix at any position is related through a similarity transformation to the one turn matrix at any other position. The spin tune ν_{sp} is defined to be this angle divded by 2π. The axis of the rotation is denoted by a unit vector $\mathbf{n}(\theta)$. A particle whose spin is aligned with $\mathbf{n}(\theta)$ at any θ will remain aligned with $\mathbf{n}(\theta)$ for all θ. Given $M(\theta)$ the spin tune and the precession axis can be determined from the relations:

$$\cos(\pi\nu_{sp}) = \frac{(TrM)}{2}, \quad \text{and} \quad \mathbf{n} = \frac{i}{2\sin(\pi\nu_{sp})} Tr(\vec{\sigma}M). \tag{52}$$

This may be verified by writing

$$M = \exp(-i\vec{\sigma}\cdot\mathbf{\Omega}) = \cos(|\Omega|/2) - i\vec{\sigma}\cdot\mathbf{\Omega}\sin(|\Omega|/2), \tag{53}$$

forming the quantities specified and taking the traces.

The idea of a Siberian Snake was described by Derbenev and Kondradenko[9] in '74. The snake described by Fig. 9 is designated a Type I snake. Assume there is a spin rotator designated S that rotates the spin 180° about the longitudional axis. The top sketch of Fig. 9 begins at position A and follows an up vertical spin around the ring. It comes back to position A pointing down (drawn with dashes and designated by a number 2). The middle sketch follows a horizontal spin, and the bottom sketch follows a longitudinal spin. The angle designated θ in these drawings is the angular precession traveling from A to B (modulo 2π), and A is chosen so that this is the same angle as going from C to A. The net outcome is rotation of 180° about the longitudinal axis, independent of θ. In other words the spin tune is one-half for all energies! This can also be verified by calculating Tr M. For this ring (letting $\nu = \gamma a$)

$$\begin{aligned} M &= \exp\left(\tfrac{-i\pi}{2}\nu\sigma_z\right)\exp\left(\tfrac{-i\pi}{2}\nu\sigma_y\right)\exp\left(\tfrac{-i\pi}{2}\nu\sigma_z\right) \\ &= \exp\left(\tfrac{-i\pi}{2}\nu\sigma_y\right)\exp\left(\tfrac{+i\pi}{2}\nu\sigma_z\right)\exp\left(\tfrac{-i\pi}{2}\nu\sigma_z\right) \\ &= \exp\left(\tfrac{-i\pi}{2}\nu\sigma_y\right) = -i\sigma_y. \end{aligned} \tag{54}$$

Hence Tr M = $\cos(\pi\nu_{sp}) = 0$, implying $\nu_{sp} = 1/2$.

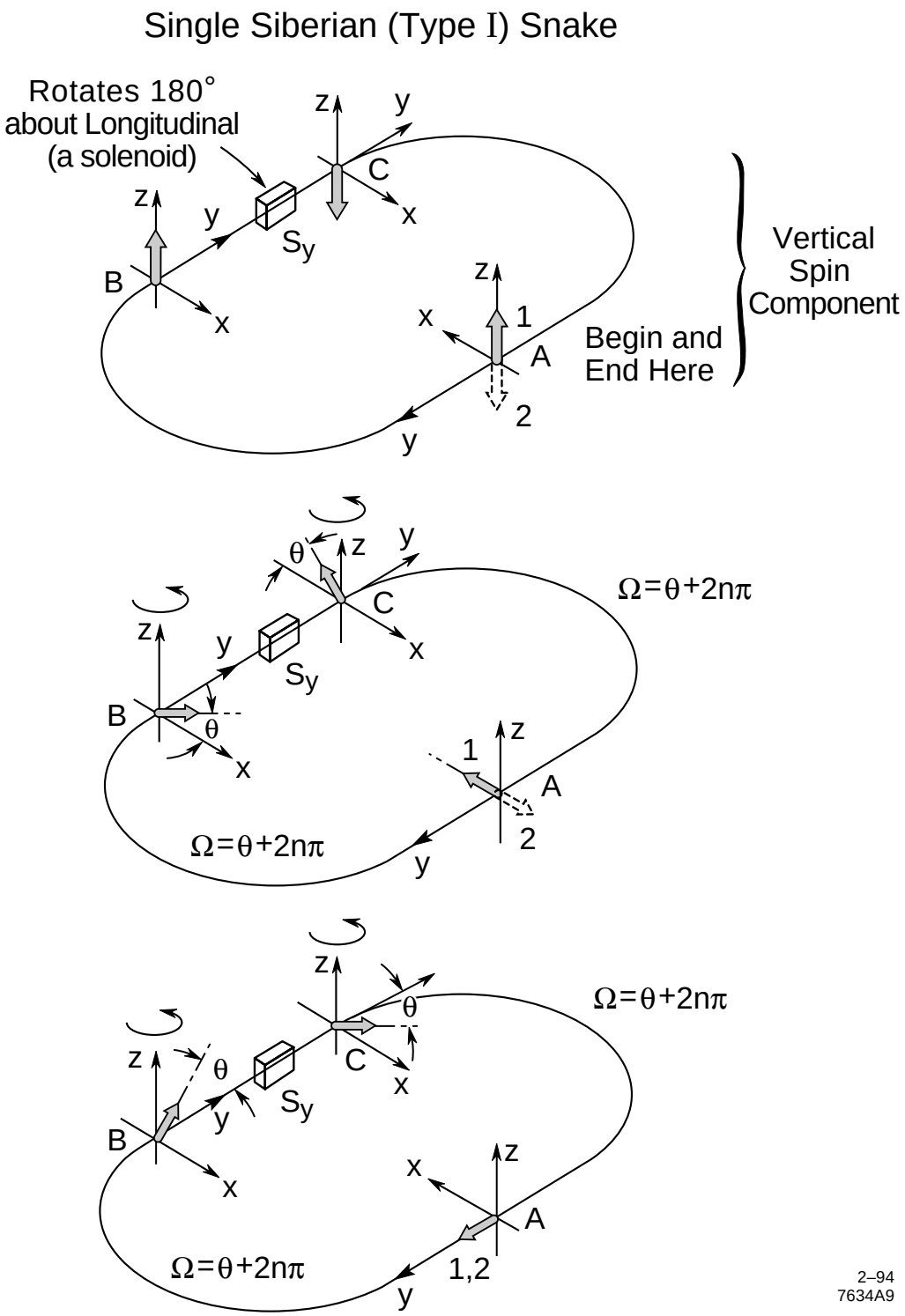

Figure 9. Sketches showing the progression of polarization axes in a type I siberian snake.[8]

The type I snake has the defect that the rotation axis $\mathbf{n}(\theta)$ is in the horizontal plane. The type II snake shown in Fig. 10 does not have this problem. This ring contains two rotators, one which rotates 180° about the longitudinal and another

which rotates 180° about the vertical. This snake has $\nu_{sp} = 1/2$, and the axis $\mathbf{n}(\theta)$ is up for one-half of the ring and down for the other half. For this ring

$$\begin{aligned} M &= \exp\left(\tfrac{-i\pi}{2}\sigma_x\right)\exp\left(\tfrac{-i\pi}{2}\nu\sigma_z\right)\exp\left(\tfrac{-i\pi}{2}\sigma_y\right)\exp\left(\tfrac{-i\pi}{2}\nu\sigma_z\right) \\ &= \exp\left(\tfrac{-i\pi}{2}\sigma_x\right)\exp\left(\tfrac{\pm i\pi}{2}\sigma_y\right) \\ &= (i\sigma_x)\,(i\sigma_y) = -i\sigma_z. \end{aligned} \tag{55}$$

Hence again $TrM = cos(\pi\nu_{sp}) = 0$, and $\nu_{sp} = 1/2$.

Apparently, if resonance widths are less than $1/2$ then the spin should never go through a resonance. There are two effects which complicate this simple picture. When sextupoles and octupoles are included, the fourier anlaysis of orbits has components at frequencies other than the integers (k), and $k \pm \nu_z$ as indicated above following Eq. 46. There are also components at $k + k_z\nu_z + k_x\nu_x + k_s\nu_s$, where k, k_z, k_x, and k_s are all integers. Hence, there is potentially a resonance condition with a snake whenever

$$1/2 = k + k_z\nu_z + k_x\nu_x + k_s\nu_s. \tag{56}$$

Figure 11 shows the possible location of such resonances in the (ν_x, ν_z) tune plane taking $k = k_s = 0$ and $\mid k_z \mid + \mid k_x \mid \leq 2$. These nonlinear resonances could apparently be avoided with proper choice of the betatron working tune (ν_x, ν_z).

There is another effect: the presence of errors can shift the tune spin from $1/2$. Suppose the particle is being accelerated through a resonance and $\nu = \gamma a = k$. Then, using Eqs. 41 and 43,

$$M\,(\theta_1 \rightarrow \theta_2) = \exp\left(-i\frac{k\,(\theta_2 - \theta_1)}{2}\sigma_z\right)\exp\left(\frac{-i\vec{\varepsilon}\cdot\vec{\sigma}\,(\theta_2 - \theta_1)}{2}\right), \tag{57}$$

since $\lambda_z = 0$, $\lambda_x = \mid \varepsilon \mid cos\varphi$, $\lambda_s = \mid \varepsilon \mid sin\varphi$. For one turn of the type I snake

$$\begin{aligned} M &= \exp\left(\tfrac{-i\pi}{2}k\sigma_z\right)\exp\left(\tfrac{-i\pi}{2}\vec{\varepsilon}\cdot\vec{\sigma}\right)\exp\left(\tfrac{-i\pi}{2}\sigma_y\right)\exp\left(\tfrac{-i\pi}{2}k\sigma_z\right)\exp\left(\tfrac{-i\pi}{2}\vec{\varepsilon}\cdot\vec{\sigma}\right) \\ &= \exp\left(\tfrac{-i\pi}{2}k\sigma_z\right)\exp\left(\tfrac{-i\pi}{2}\vec{\varepsilon}\cdot\vec{\sigma}\right)\exp\left(\tfrac{\pm i\pi}{2}k\sigma_z\right)\exp\left(\tfrac{-i\pi}{2}\sigma_y\right)\exp\left(\tfrac{-i\pi}{2}\vec{\varepsilon}\cdot\vec{\sigma}\right) \\ &= \exp\left(\tfrac{\pm i\pi}{2}\vec{\varepsilon}\cdot\vec{\sigma}\right)\exp\left(\tfrac{-i\pi}{2}\sigma_y\right)\exp\left(\tfrac{-i\pi}{2}\vec{\varepsilon}\cdot\vec{\sigma}\right), \end{aligned} \tag{58}$$

where the + sign holds for odd k and the – sign for even k. This can be further

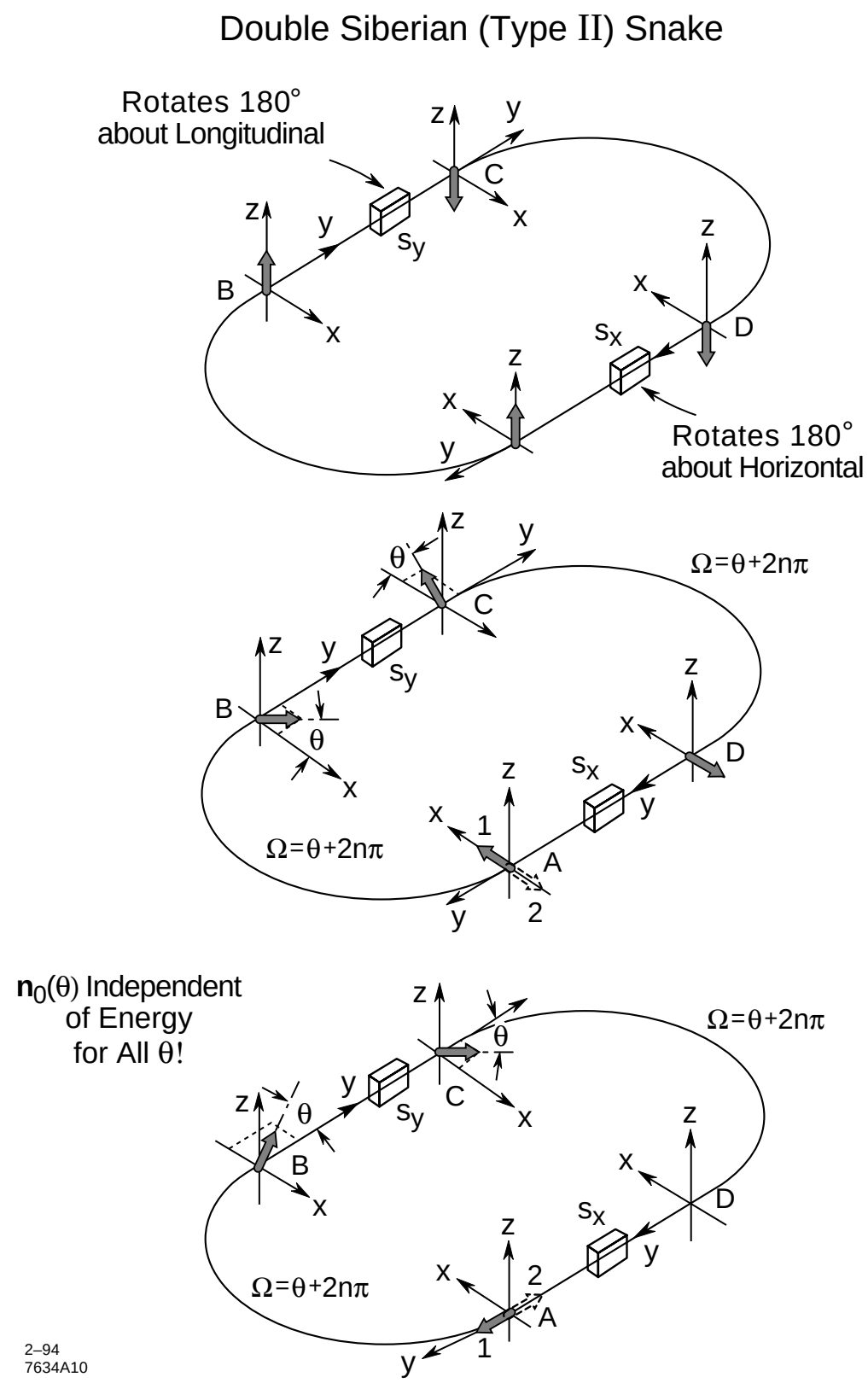

Figure 10. Sketches showing the progression of polarization axes in a type II siberian snake.[8]

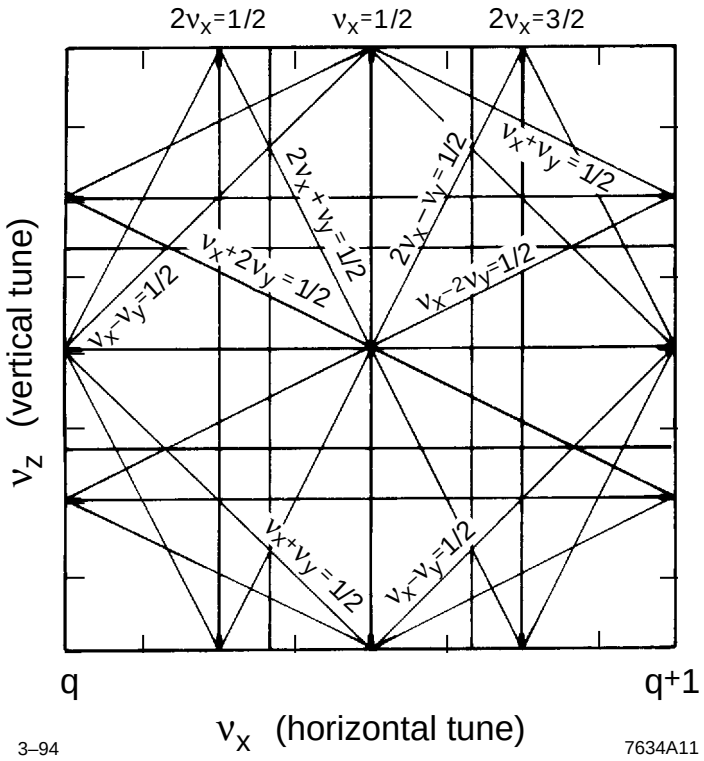

Figure 11. A diagram of the the betatron tune plane showing nonlinear resonant conditions in the presence of a siberian snake. There could also be synchrotorn sidebands to these resonances.[10]

reduced to

$$M = \exp\left(\frac{\pm i\pi}{2}\vec{\varepsilon}\cdot\vec{\sigma}\right)\exp\left(\frac{-i\pi}{2}\vec{\varepsilon}_T\cdot\vec{\sigma}\right)(i\sigma_y)\,, \tag{59}$$

where $\varepsilon_T = (-\varepsilon_x, \varepsilon_y)$. Expanding the exponential and taking the trace one finds

$$\begin{aligned} \tfrac{1}{2}TrM &= \tfrac{1}{2}Tr\ \ -\sin(\pi\,|\varepsilon|)\,(\pm\vec{\varepsilon}\cdot\vec{\sigma} - \vec{\varepsilon}_T\cdot\vec{\sigma})\,\tfrac{\sigma_y}{|\varepsilon|} \\ &= \{0\ if\ k\ odd,\ \sin\varphi\sin(\pi|\varepsilon|)\ if\ k\ even\}. \end{aligned} \tag{60}$$

Hence $\nu_{sp} = 1/2$ for k odd but could lie in a band from $1/2 - \mid\varepsilon\mid < \nu_{sp} < 1/2 + \mid\varepsilon\mid$ for k even. Of course an arbitrary integer could also be added to the tune. This would suggest that this snake would be effective if $\mid\varepsilon\mid < 1/2$.

Following the same analysis with the type II (double snake) leads to

$$\cos(\pi\nu_{sp}) = -\cos 2\varphi\sin^2(\pi\,|\varepsilon|/2)\,, \tag{61}$$

which cannot have an integer ν_{sp} if $\mid\varepsilon\mid < 1$. Multiple double snakes lead to the

condition

$$\cos(\pi\nu_{sp}/N) = -\cos 2\varphi \sin^2(\pi\,|\varepsilon|/N)\,. \tag{62}$$

This equation will have no integer solution if $sin^2(\pi \mid \varepsilon \mid /N) < sin(\pi/2N)$, which implies a condition

$$|\varepsilon| < \quad \overline{2N/\pi} \tag{63}$$

This suggests that the number of snakes must increase as the square of the resonance width. There is some debate in the literature on this point, and other estimates yield a limit that increases linearly with the resonance width. The latest estimate is that 26 double snakes would be required in the SSC to ensure absence of spin resonances.[11] Of course there is also the requirement of a properly chosen working tune to avoid nonlinear resonances.

A nice sequence of experiments has been performed with siberian snakes at the University of Indiana cyclotron facility. Krisch et al ('89)[12] and J. Goodwin ('90)[13] published results showing that the type I snake performed as expected. Also M. Minty, ('91)[14] verified that a type I snake removed resonance behavior for imperfection, betatron, and synchrotron resonances. Results are illustrated in Fig. 12.

Overlapping resonances have also been recently investigated at this facility by Baiod et al. ('93),[15] with an rf resonance overlapping an imperfection resonance. The snake was effective in removing the depolarization that occurred without the snake. See Fig. 13.

5 Electron Rings

5.1 Characteristic Times

Figure 14 shows the characteristic times for different processes that occur in electron storage rings. The ring of this example has an energy of 25 GeV, but these times may be easily scaled to other energies using the fact that the radii of these rings scale like the second power of energy ($\rho \sim \gamma^2$). The photon energy radiated per second for a particle in a constant magnetic field is given classically

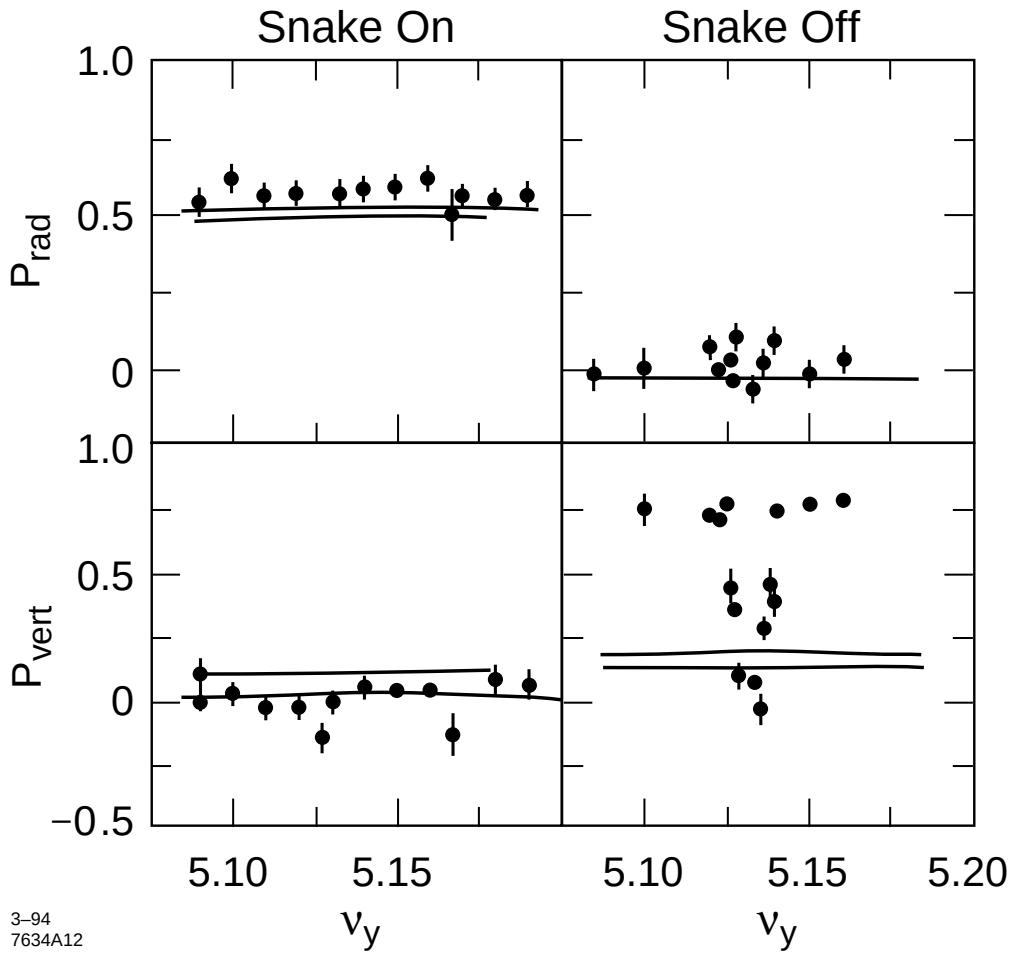

Figure 12. Experiment at the Indiana Univerty Cycltron Facility showing the preservation of polarization with a snake. (Note: Injected polarization was horizontal with the snake on, and vertical with the snake off.[14])

by

$$\frac{dU}{dt} \equiv P_\gamma = \frac{2}{3}\frac{cr_e}{\rho^2}mc^2\gamma^4 \quad (\sim 1)\,, \tag{64}$$

and the so called critical energy for these photons is

$$\hbar\omega_c = \frac{2}{3}\frac{\lambda}{\rho}mc^2\gamma^3 \quad (\sim \gamma)\,.$$

The average photon energy is about 0.3 times the critical energy. An important ratio, the critical energy divded by the particle energy, is indepedent of energy and has a value of about 10^{-6}:

$$\xi = \frac{\hbar\omega_c}{E} = \frac{2}{3}\frac{\lambda}{\rho}\gamma^2 \approx 10^{-6} \quad (\sim 1)\,.$$

The number of photons radiated per second is P_γ divided by the average photon

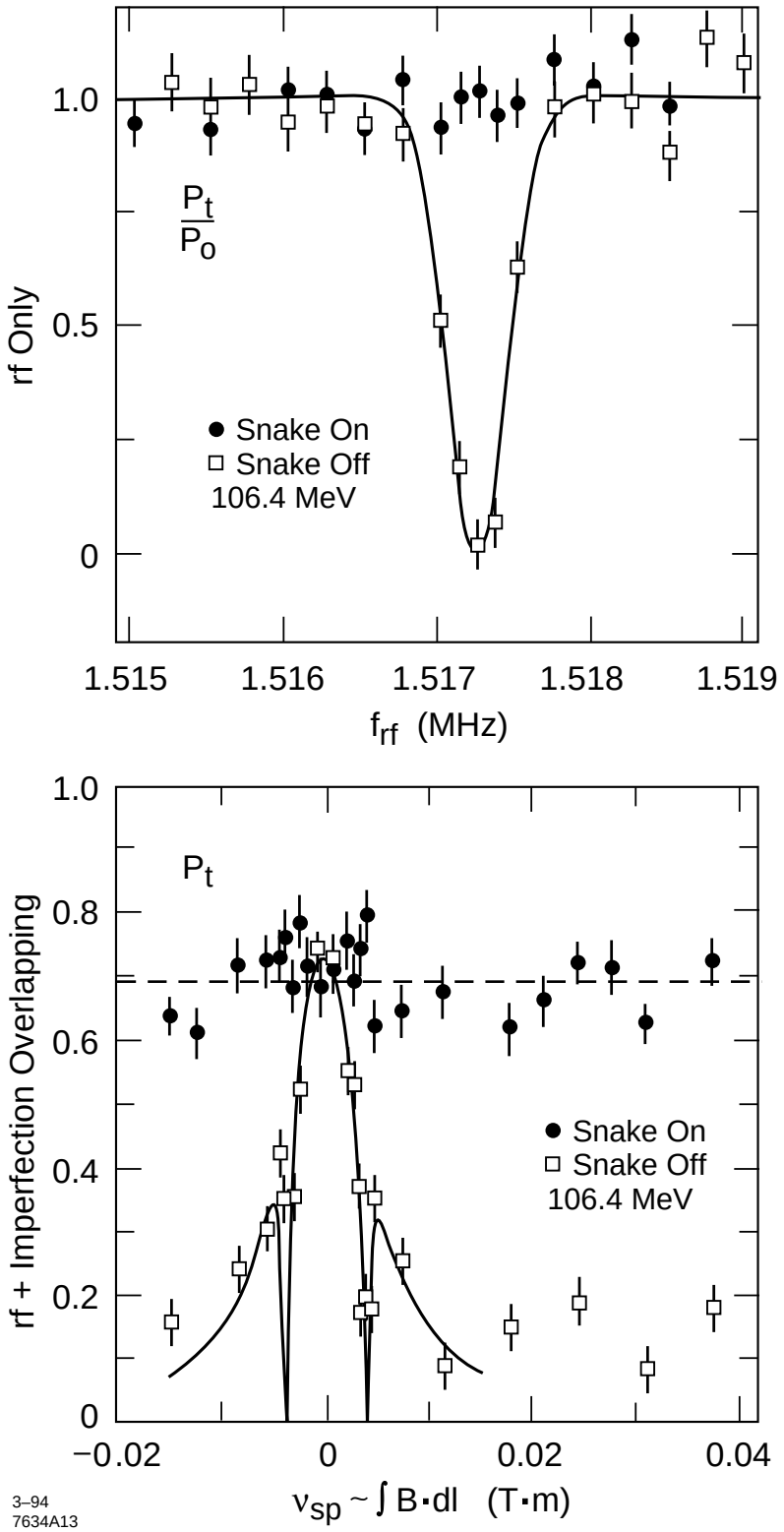

Figure 13. Experiment at the Indiana Univerty Cyclotron Facility showing the preservation of polarization with a snake in the case of overlapping resonances.[15]

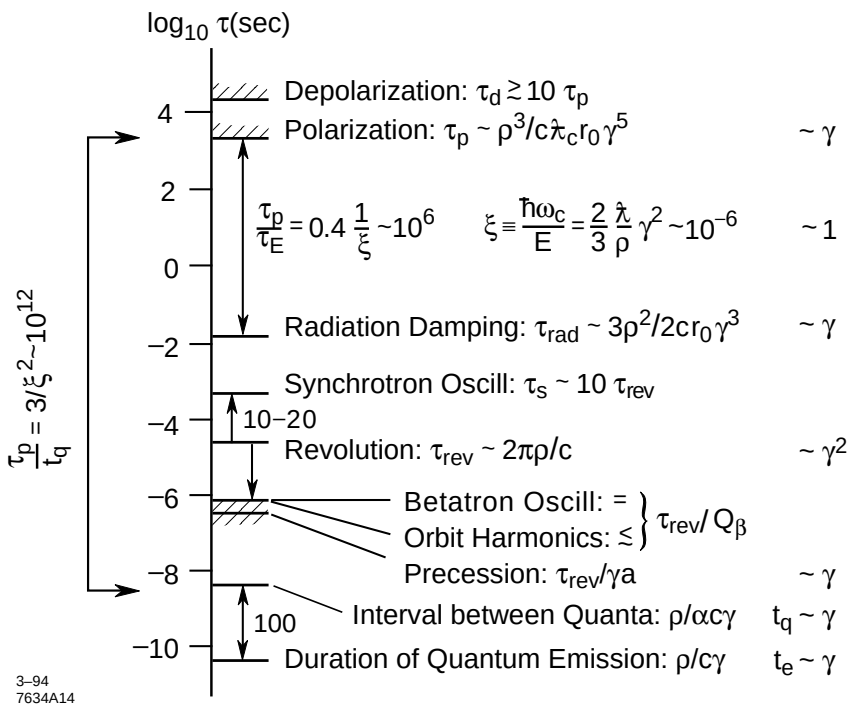

Figure 14. Characteristic times of a 25 GeV electron storage ring.[8]

energy:

$$\frac{dN}{dt} = \frac{5\sqrt{3}}{6}\frac{\alpha c}{\rho}\gamma \quad (\sim \gamma^{-1}) .$$

The number of seconds per quanta radiated in the inverse of this number radiated per second is

$$t_\gamma = \frac{2\sqrt{3}}{5}\frac{\rho}{\alpha c\gamma} \quad (\sim \gamma) .$$

The duration time of an emission process is given by

$$t_e = \frac{\rho}{c\gamma} \quad (\sim \gamma) .$$

This is the time in which the angular change in orbit direction is $1/\gamma$, and $t_\gamma/t_e = 2\sqrt{3/(5\alpha)} \approx 100$. In other words the emission time is always much shorter than the time between emissions. Of course the revolution time is

$$\tau_R = \frac{2\pi\rho}{c} \quad (\sim \gamma^2) .$$

The spin precession rate is γa per period, so the time for one precession is $\tau_R/\gamma a$.

The energy oscillation (synchrotron oscillations) damping time is given by the particle energy divided by the rate of radiated photon energy:

$$\tau_E = \frac{E}{P_\gamma} = \frac{3}{2}\frac{\rho^2}{r_e c \gamma^3} \quad (\sim \gamma)\,.$$

The damping time for the betatron oscillations is two times the energy damping time:

$$\tau_x = 2\tau_E \quad (\sim \gamma)\,.$$

5.2 Self Polarization

Sokolov and Ternov[16] found that the spin-flip transition rate during synchrotron radiation depends on the direction of the spin. The spin-flip transition rate is given by

$$W = \frac{1}{2\tau_p}\left[1 + \frac{8\sqrt{3}}{15}(\mathbf{n}\cdot\hat{\mathbf{z}})\right],$$

where

$$\tau_p = \frac{8\sqrt{3}}{15}\frac{\rho^3}{\lambda c r_e \gamma^5} \quad (\sim \gamma)\,.$$

The down state is preferred over the up state, and in the steady state the beam will have obtained a polarization

$$P_{\max} = \frac{W^{\uparrow\downarrow} - W^{\downarrow\uparrow}}{W^{\uparrow\downarrow} + W^{\downarrow\uparrow}} = \frac{8\sqrt{3}}{15} \approx 0.92$$

Baier, Katkov, and Strakhovenko[17] found an additional term for the case in which the polarization has a component in the direction of the beam.

$$W = \frac{1}{2\tau_p}\left[1 + \frac{8\sqrt{3}}{15}(\mathbf{n}\cdot\hat{\mathbf{z}}) - \frac{2}{9}(\mathbf{n}\cdot\hat{\mathbf{s}})^2\right];$$

$(\mathbf{n}\cdot\hat{\mathbf{s}})$ is usually quite small.

If the beam is completely unpolarized at time $t = 0$, the polarization will grow according to the formula

$$P(t) = -\frac{B}{A}\left(1 - e^{-At}\right),$$

where

$$A = \left\langle \frac{1}{\tau_p}\left(1 - \frac{2}{9}\left(\mathbf{n}(\theta)\cdot\hat{\mathbf{s}}\right)^2\right)\right\rangle \quad \text{and} \quad B = \left\langle \frac{1}{\tau_p}\left(\mathbf{n}(\theta)\cdot\hat{\mathbf{b}}\right)^2\right\rangle.$$

Here $\hat{\mathbf{b}}$ is a unit vector in the direction of the magnetic field component perpendicular to $\mathbf{s}$. The average is taken over the closed orbit. Recall that $\mathbf{n}(\theta)$ is the axis of the one turn rotation matrix. The beam will polarize in this direction. The charactieristic polarization time is τ_p, also shown in Fig. 14. It is much longer than most other characteristic times.

5.3 Spin Diffusion and Depolarization

In addition to a polarization mechanism, there is a depolarization mechanism. Whether the beam actually polarizes depends on the relative rates of the these processes.

When a particle emits a photon it changes energy discontinuously. Particles of the new energy have a different closed orbit, so the particle is all of a sudden not on the closed orbit, and will begin to execute oscillations about the new closed orbit. The derivative of the closed orbit with frational change in energy is called the dispersion vector $\vec{\eta}(s)$. Since the position and slope of the orbit do not change during the emission process, the amplitude of the betatron oscilation is given by $\mathbf{z}_0 = -\vec{\eta}(s_o)\delta_o$ (this is a phase space four component vector), where s_o is the position in the ring at which the quanta was emitted, and δ_o is the fractional change in energy. In a perfectly planar ring the dispersion vector will lie in the horizontal plane, and the betatron oscillation will also lie in this plane. In such a case the particle would experience no horizontal fields, and the polarization vector will remain unchanged. However in real rings, because of quadrupole misalignments and slight tilting of bend and quadrupole magnets, the dispersion vector has vertical components, and the horizontal and vertical betatron motion are slightly coupled. The analysis of Section 3.2 concludes that even in such a situation the betatron motion can be completely described by four functions.

Though impossible, assume for a moment that the betatron amplitude after emission was zero. Then the motion would be along a deviated closed orbit described by $\vec{\eta}(s)\delta$. As the particle travels along this orbit it may encounter a small horizontal field, say in a displaced quadrupole. This rotates the spin slightly about the horizontal axis, creating a very small component of spin in the longitudinal direction. Micro-radians will be shown later to be the relevant rotation scale. Continuing around the ring to the starting point, this small component of spin precesses, until at the end of the first turn, though it will lie in the horizontal plane, it will have components both perpendicular and parallel to the direction of motion of the orbit. Other displaced quadrupoles would similarly contribute a spin component in the horizontal plane. Since these contributions are so very small, the spin vector at each small horizontal field is almost vertical. Hence all of the horizontal vector components can be taken to add linearly. Let the sum of all these horizontal components be $\delta\mathbf{S}_1$.

On the second turn two things will have happened: i) the energy will have changed slightly and will begin following a synchrotron oscillation, so that on subsequent turns the energy will be given by $\delta_j = cos(j\mu_s)\delta_o$, and ii) the energy will have decreased very slightly due to further radiation. Taken together $\delta_j = exp(-j\tau_R/\tau_E)cos(j\mu_s)\delta_o$. The ratio $1/N = \tau_R/\tau_E$ is typcially between 10^{-3} and 10^{-4}. Thus the contribution to the horizontal spin on the second turn is $\delta\mathbf{S}_1 = e^{-1/N}cos(\mu_s)\delta\mathbf{S}_1$. To this must be added the contribution of the first turn which will have precessed by $2\pi\nu_{sp} = 2\pi\gamma a \equiv \mu_{sp}$. Representing the horizontal spin vectors by complex numbers, and letting $\delta\mathbf{S}_1 = \varepsilon e^{i\varphi}$; it follows that $\delta\mathbf{S}_2 = exp(-1/N)cos(\mu_s)\varepsilon e^{i\varphi}$, and the total horizontal spin after two turns will be

$$\delta\mathbf{\Sigma}_2 \equiv \delta\mathbf{S}_1 e^{i\mu_{sp}} + \delta\mathbf{S}_2 = \left(1 + e^{-1/N}\cos(\mu_s)\, e^{-i\mu_{sp}}\right)\varepsilon e^{i(\varphi+\mu_{sp})}.$$

After j turns

$$\begin{aligned}\delta\mathbf{\Sigma}_j &\equiv \delta\mathbf{S}_1 e^{ij\mu_{sp}} + \delta\mathbf{S}_2 e^{i(j-1)\mu_{sp}} + \ldots + \delta\mathbf{S}_j \\ &= \left(1 + e^{-1/N}\cos(\mu_s)\, e^{-i\mu_{sp}} + \ldots + e^{-j/N}\cos(j\mu_s)\, e^{-ij\mu_{sp}}\right)\varepsilon e^{ij(\varphi+\mu_{sp})}\end{aligned}$$

Because of the small damping the infinte sum can be carried out, then the limit

$N \to \infty$ can be taken:

$$\delta \mathbf{\Sigma}_{j\to\infty} \to \varepsilon e^{ij(\varphi+\mu_{sp})} \frac{1}{2} \left\{ \left[1 - e^{i(\mu_s-\mu_{sp})}\right]^{-1} + \left[1 - e^{i(-\mu_s-\mu_{sp})}\right]^{-1} \right\}$$
$$= \frac{i}{4} \varepsilon e^{ij\varphi+(j-1/2)\mu_{sp}} \left\{ \frac{e^{i\mu_s/2}}{\sin\left((\mu_{sp}-\mu_s)/2\right)} + \frac{e^{-i\mu_s/2}}{\sin\left((\mu_{sp}+\mu_s)/2\right)} \right\}.$$

A non-zero horizontal component of the spin is left which is precessing about the vertical. Note the denominators which vanish when $\mu_{sp} = \pm\mu_s$. This is typical, and illustrates a large depolarization at this resonance condition. Away from the resonance the sum has the order of magnitude of the first turn contribution to the spin which should be very small for reasons mentioned above plus the fact that all of the contributions from the quadrupoles around the ring also will tend to cancel one another. Note that if $\delta\mathbf{S}_1$ had been calculated starting at a different place along the orbit, the value of ε would remain unchanged, and φ would advance by $\nu_{sp}s/C$ around the ring. The magnitude of ε is proportional to δ, the energy fraction of the radiated photon.

The betatron motion can be treated in exactly the same way. In this case there are four contributions: two modulated by the horizontal betatron tune, and two modulated by the vertical betatron tune. Letting $\mathbf{z}$(s) be the phase space vector of Section 2.2, and A the matrix found from the eigenvectors of the one-turn matrix, the motion resulting from the quantum emission will be given by

$$\mathbf{z}\,(s) = \Sigma_k\ \mathbf{z}_k\,(s)\,q_k,$$

where q_k may be found from

$$\mathbf{q} = -\mathbf{A}\vec{\eta}\delta.$$

In this case it is required to find the contribution to the horizontal spin vector that accrues along the first turn trajectory defined by $\mathbf{z}_k(\tilde{s})$. Later turn contributions are modulated by $\cos(j\mu_x)$, $\sin(j\mu_x)$, $\cos(j\mu_y)$, or $\sin(j\mu_y)$ just as the closed orbit example was moulated by $\cos(j\mu_s)$. The contribution of each can be summed, then added together and to the closed orbit sum, to give the total change in the spin vector as the result of the quantum emission. Each contribution is proportional

δ, the energy fraction emitted. Derbenev and Kontratenko[18] define a vector , , which they call the spin-orbit coupling function, by

$$\delta \mathbf{n} = \mathbf{\Gamma} \delta,$$

where $\delta \mathbf{n}$ is the small rotation vector that would give the horizontal spin component $\delta \Sigma_\infty$ (summing together betatron and closed orbit contributions). As a result of N repeated emissions there will be a random walk in the horizontal vector $\mathbf{n}$ given by

$$\mid \Delta \mathbf{n} \mid = \mid \Sigma (\delta \mathbf{n})^2 \mid^{1/2} = \left[N, {}^2\delta^2 \right]^{1/2}.$$

During a polarization time τ_p there are $N = \tau_p / \tau_q = 3/\xi^2$ emissions (recall $\xi = \hbar \omega_c / E \approx 10^{-6}$). Also $\delta \approx \hbar \omega_c / E = \xi$. Hence in a polarization time, $\mid \Delta \mathbf{n} \mid \approx \sqrt{3} \mid \mathbf{\Gamma} \mid$. To achieve a polarized beam, $\mid \mathbf{\Gamma} \mid$ should be small compared to unity, implying the one-turn $\delta \mathbf{n} (= \mathbf{\Gamma} \delta)$ must be small compared to 10^{-6}.

The polarization time development will now follow the equation

$$P(t) = -\frac{B}{A} \left(1 - e^{-At} \right),$$

with

$$A = \left\langle \frac{1}{\tau_p} \left(1 - \frac{2}{9} \left(\mathbf{n}(\theta) \cdot \mathbf{s} \right)^2 + \frac{11}{18} \mid \mathbf{\Gamma} \mid^2 \right) \right\rangle \quad \text{and} \quad B = \left\langle \frac{1}{\tau_p} \left(\mathbf{n}(\theta) \cdot \mathbf{b} \right)^2 \right\rangle.$$

Unfortunately the theory described above is not adequate to totally explain the depolarization measurements; a theory which includes nonlinear effects is required. The details of such a theory are beyond the scope of these lectures, but they proceed very much like the linear theory. Normal form theory establishes that there are four variables (as $\mathbf{q}$ above, which reside in a 2-degrees-of-freedom phase space) which determine the orbit at some starting position and which advance turn-by-turn according to a block diagonal rotation, as in the linear theory. The particle position along the orbit can be expanded as a power series in these variables, the coefficients being functions of the distance along the orbit. So just as in the linear theory, a set of functions (the coefficients of the power series mentioned) for one revolution determine the orbit for all revolutions. The contribution to

the change of the spin vector of each term of the power series can be calculated, much as for the linear theory, taking into account that for some magnets, like sextupoles, the horizontal magnetic field may be a quadratic or a higher power of the position variable. Thus a contribution to the change in spin vector comes to be modulated by a higher power of the rotation functions, e.g., $\cos^2(n\mu_x)$. The infinite sum of such terms will contain a denominator that is zero for a condition like $\nu_{sp} \pm 2\nu_x = n$.

There are computer codes which calculate $\mathbf{\Gamma}$. In order of increasing sophistication and date of development, examples are SLIM,[19] SMILE,[20] and SODOM.[21]

Figure 15a shows depolarization data from SPEAR[22] A curve was fit through the data points to aid the eye, and resonance locations were identified. There is clear evidence of nonlinear resonances. Figure 15b shows the results of nonlinear theory as computed by S. Mane.[23] The fit is remarkably good. Some resonances were identified with this fit that were not explicitly called out in the original data analysis.

5.4 Beam Energy Measurements

Using spin depolarization to measure beam energy was first suggested by Serednyakov ('76).[24] A fast kicker magnet with a horizontal magnetic field is inserted into the ring. If the phase advance per turn of the kicker magnetic field ($2\pi\nu_{dep}\tau_R$) equals the phase advance of the spin ($2\pi\nu_{sp}$) plus or minus an integer multiple of $2\pi(\pm 2\pi n)$, then the spin should be depolarized by the kicker. This equation can be written

$$\nu_{dep} = (\nu_{sp} \pm n)\,\nu_R,$$

where ν_{dep} and ν_R can be measured accurately, and since $\nu_{sp} = \gamma a$, and a is known accurately, an accurate value for γ is obtained. The data shown in Fig. 16 were taken at Doris ('83).[25] The energy is determined to a part in 10^5. Similar measurements were performed in Novosibirsk,[26] and it is standard operating procedure at LEP to perform this measurment several times per week.[27] To perform the measurement at LEP it is necessary to move some 880 MeV off of the Z_0 peak, slightly change the tunes, install some bumps to compensate the solenoid, and dump the e^+ beam. An interesting side note is that a periodic variation in the energy was observed which was ultimately attributed to the tides of the moon.[28]

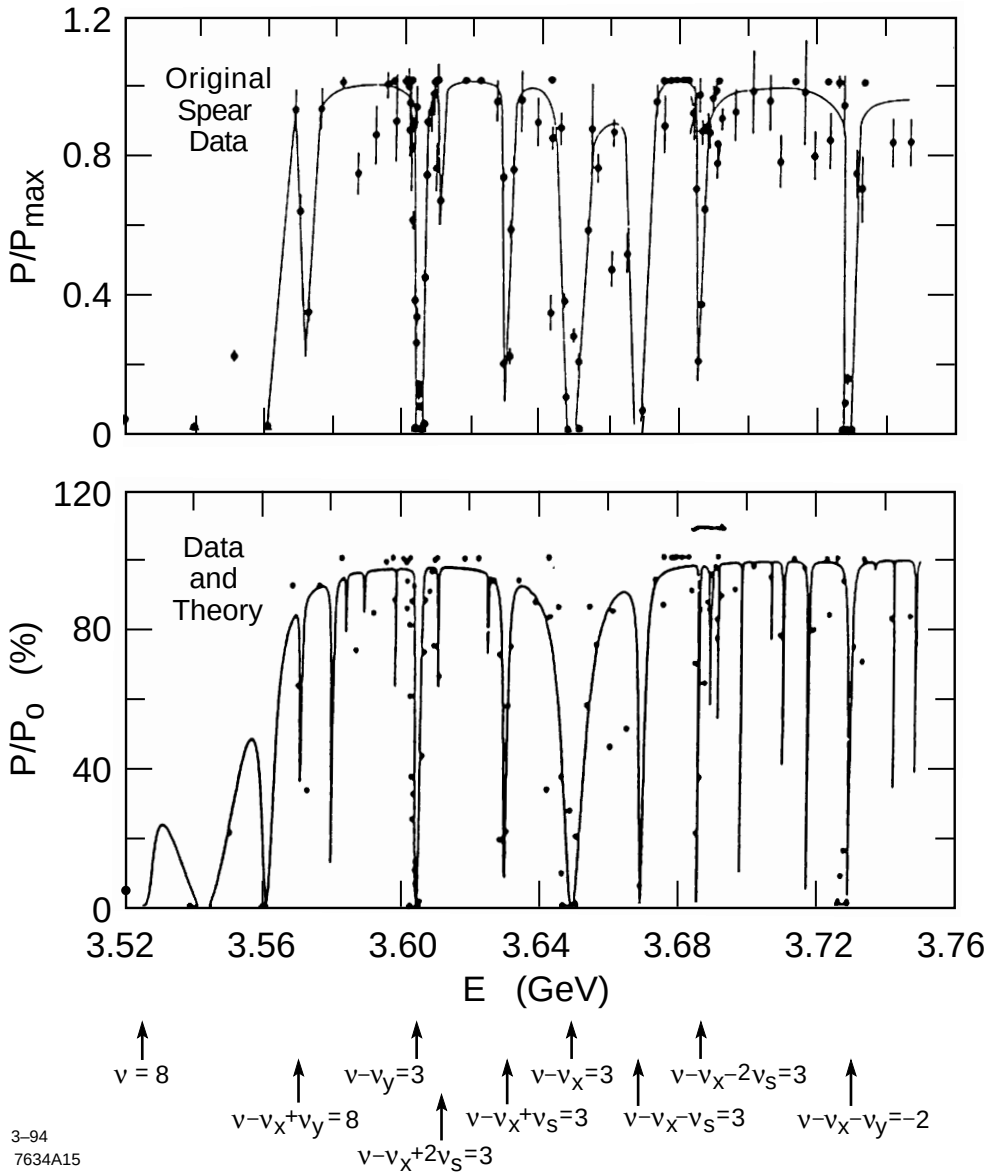

Figure 15. SPEAR depolarization data[22] and theoretical calculations of depolarization by S. Mane.[23]

The polarization time is very long at LEP, on the order of three hours. A number of refinements, namely improved orbit measuerement and magnet realignment, harmonic spin matching, change in phase advance per cell in the vertical plane optics, and an improved polarimeter have resulted in an assymptotic polarization of perhaps 40% to 50%.

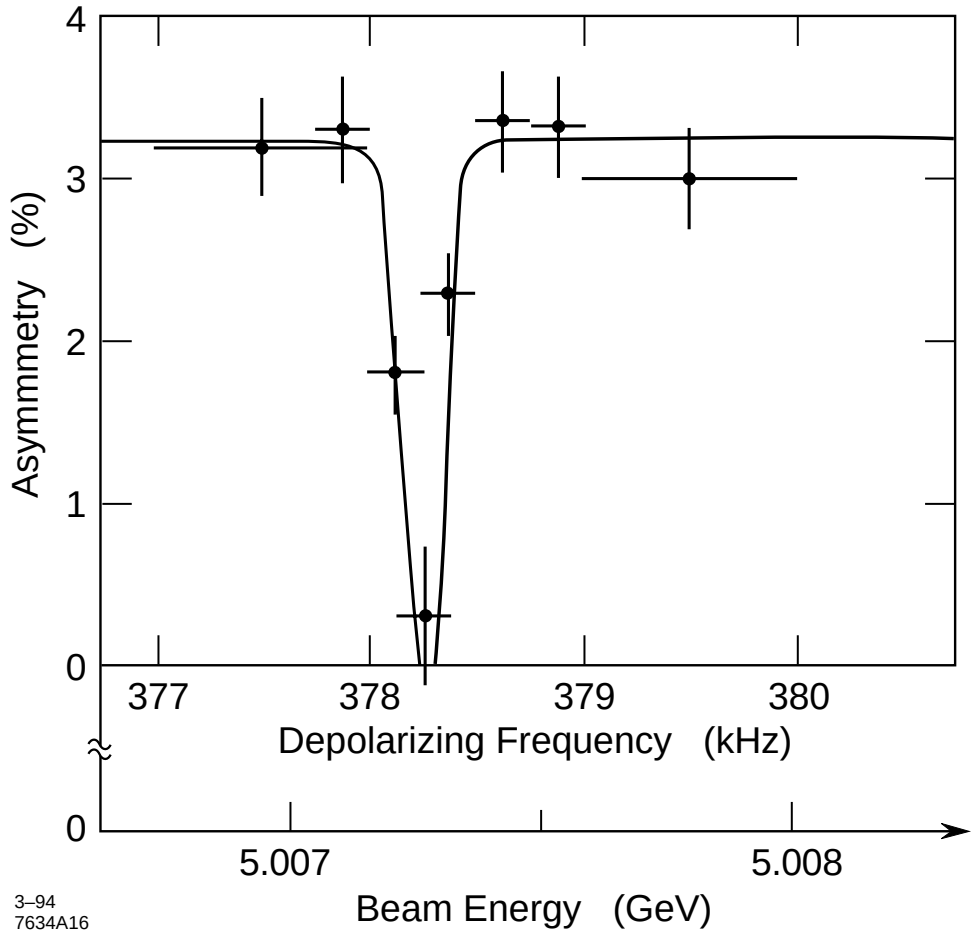

Figure 16. Energy measurment at DORIS using spin depolarization by a high frequency vertical kicker magnet.[25]

6 Acknowledgements

I thank R. Ruth and M. Minty for several helpful discussions and for providing access to their extensive spin-literature collections. I also thank M. Minty for serving as a fine "provocateur" for these lectures and thereby improving their depth.

References

[1] V. Bargman, L. Michel, and V. L. Telegdi, Phys. Rev. Lett. **2** (1959).

[2] L. H. Thomas, Philos. Mag. (1927).

[3] W. Panofsky and M. Schwarz, SLAC–CN–361 (1987).

[4] T. Limberg and P. Emma, "The north arc of the SLC as a spin rotator," SLAC–PUB–6210 (1993).

[5] E. Courant and R. Ruth, "The acceleration of polarized protons in circular accelerators," BNL–51270 (1980).

[6] M. Minty, "Electron beam depolarization in a damping ring," SLAC–PUB–6114 (1993).

[7] M. Froissart and R. Stora, Nucl. Instr. Meth. (1960).

[8] B. Montague, "Polarized beams in high energy storage rings," Physics Reports **113**, 1 (1984).

[9] Ya. Derbenev and A. Kondratenko, in Procedings of the 10th International Conference on High Energy Accelerators, Protvino, V.2, p.70 (1977) [Siberian snake idea].

[10] R. Ruth, "The Acceleration and Storage of High Energy Polarized Protons," CERN LEP–TH/83–47 (1983).

[11] K. Yokoya, "On multiple Siberian snakes," SSC–189 (1988).

[12] A. D. Krisch, "First test of Siberian snake to overcome depolarizing resonances in circular accelerator," Phys. Rev. Lett. **63**, 1137 (1989).

[13] J. Goodwin, Indiana University Thesis (1991).

[14] M. Minty, "Studies of Siberian snakes and depolarizing resonances at the Indian U. Cyclotron Facility," Thesis (1991).

[15] R. Baiod et.al., "A Siberian snake with overlapping depolarizing resonance, UM HE 92–19 (1993).

[16] A. Sokolov and I. Ternov, "On Polarization and Spin Effects in the Theory of Synchrotron Radiation," Sov. Phys. Doklady **8**, 1203 (1964).

[17] Baier, Katkov, and Strakhovenko, Sov. Phys. JETP **31** 908 (1970).

[18] Ya. Derbenev and A. Kondratenko, "Diffusion of particle spin in storage rings," Sov. Phys. JETP **35**, 230 (1972).

[19] A. Chao, "Evaluation of radiative spin polarization in an electron storage ring," Nucl. Instr. Meth. **29**, 180 (1981).

[20] S. Mane, Phys. Rev. **A36** 120 (1987).

[21] K. Yokoya, "Non-perturbative calculation of equilibrium polarization of stored electron beams," KEK Report 92–6 (1992).

[22] J. R. Johnson et al., Nucl.Instr.Meth. **A258** 261 (1983).

[23] S. Mane, "Higher order spin resoances," AIP Conf. Proc., **187** 957 (1989).

[24] S.I. Serednyakov, Sov. Phys. JETP **44** (1976).

[25] Doris, Physics Letters **B135**, V (1984).

[26] A. Artamonov et al. Phys. Lett. **B118** 225 (1982).

[27] M. Placidi and R. Rossmanith, "Transverse and longitudinal polarization in LEP," CERN LEP Note 545 (1985).

[28] G. Fischer and A. Hofmann, "Effects of Tidal Forces on the LEP Energy," Proceedings of the 2nd Workshop on LEP Performance, Chamonix, January 1992, p. 337.